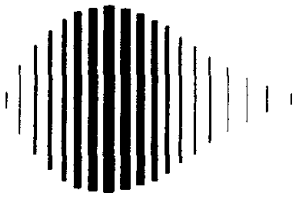

NATIONAL CENTER FOR EARTHQUAKE
ENGINEERING RESEARCH
State University of New York at Buffalo

A Multidimensional Hysteretic Model for Plastically Deforming Metals in Energy Absorbing Devices

by

E. J. Graesser and F. A. Cozzarelli
Department of Mechanical and Aerospace Engineering
State University of New York at Buffalo
Buffalo, New York 14260

Technical Report NCEER-91-0006

April 9, 1991

This research was conducted at the State University of New York at Buffalo and was partially supported by the National Science Foundation under Grant No. ECE 86-07591.

NOTICE

This report was prepared by the State University of New York at Buffalo as a result of research sponsored by the National Center for Earthquake Engineering Research (NCEER). Neither NCEER, associates of NCEER, its sponsors, State University of New York at Buffalo, nor any person acting on their behalf:

a. makes any warranty, express or implied, with respect to the use of any information, apparatus, method, or process disclosed in this report or that such use may not infringe upon privately owned rights; or

b. assumes any liabilities of whatsoever kind with respect to the use of, or the damage resulting from the use of, any information, apparatus, method or process disclosed in this report.

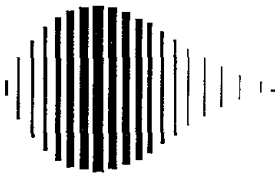

A Multidimensional Hysteretic Model for Plastically Deforming Metals in Energy Absorbing Devices

by

E.J. Graesser[1] and F.A. Cozzarelli[2]

April 9, 1991

Technical Report NCEER-91-0006

NCEER Project Number 89-2103

NSF Master Contract Number ECE 86-07591

1 ASEE/ONT Postdoctoral Fellow, David Taylor Research Center, Ship Materials Engineering Department, Annapolis, Maryland

2 Professor, Department of Mechanical and Aerospace Engineering, State University of New York at Buffalo

NATIONAL CENTER FOR EARTHQUAKE ENGINEERING RESEARCH
State University of New York at Buffalo
Red Jacket Quadrangle, Buffalo, NY 14261

PREFACE

The National Center for Earthquake Engineering Research (NCEER) is devoted to the expansion and dissemination of knowledge about earthquakes, the improvement of earthquake-resistant design, and the implementation of seismic hazard mitigation procedures to minimize loss of lives and property. The emphasis is on structures and lifelines that are found in zones of moderate to high seismicity throughout the United States.

NCEER's research is being carried out in an integrated and coordinated manner following a structured program. The current research program comprises four main areas:

- Existing and New Structures
- Secondary and Protective Systems
- Lifeline Systems
- Disaster Research and Planning

This technical report pertains to Program 2, Secondary and Protective Systems, and more specifically, to protective systems. Protective Systems are devices or systems which, when incorporated into a structure, help to improve the structure's ability to withstand seismic or other environmental loads. These systems can be passive, such as base isolators or viscoelastic dampers; or active, such as active tendons or active mass dampers; or combined passive-active systems.

Passive protective systems constitute one of the important areas of research. Current research activities, as shown schematically in the figure below, include the following:

1. Compilation and evaluation of available data.
2. Development of comprehensive analytical models.
3. Development of performance criteria and standardized testing procedures.
4. Development of simplified, code-type methods for analysis and design.

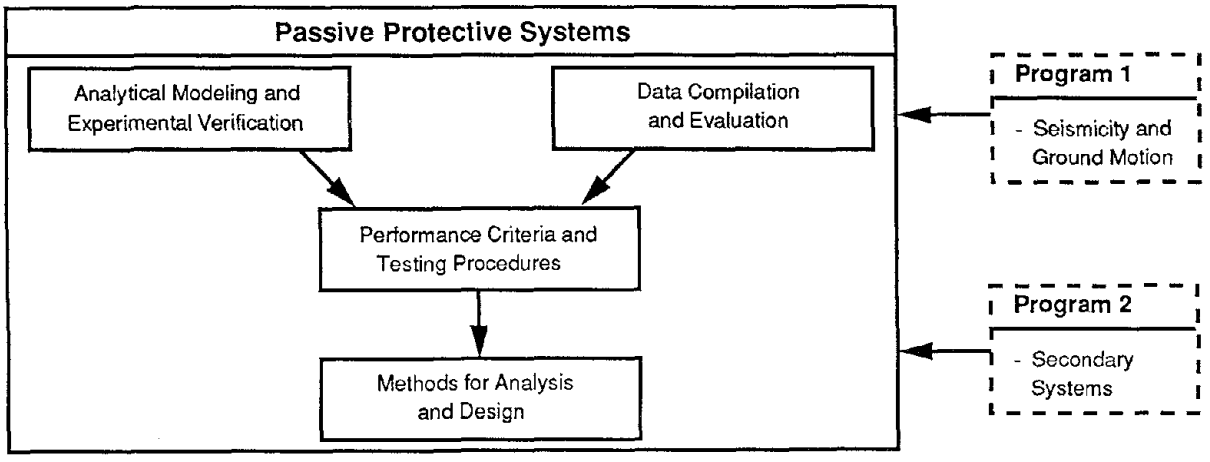

The present report is the second NCEER technical report by the same authors on the subject of modeling hysteretic materials for possible use as energy absorbing devices, the first one being NCEER-89-0018. The first report was concerned with a theoretical development of a constitutive law for shape memory alloys. This report is concerned with a new multidimensional constitutive model for plastically deforming metals, and includes a comparison with hysteretic data given in the literature.

ABSTRACT

A one-dimensional hysteretic model from the field of passive vibration control in earthquake engineering is modified so that multi-dimensional loading conditions can be included. As such, a procedure is given for extending a one-dimensional model of hysteresis to a three-dimensional tensorial representation. This is done because multi-dimensional effects and geometrical considerations are important when considering the design of a new energy absorbing device or a new damping material. The resulting model is then reduced to meet the loading conditions of three special cases; uniaxial loading, shear loading, and non-proportional biaxial loading (combined axial-torsional loading). In each of these cases the results calculated using the modeling scheme are consistent with experimentally observed behavior in plastically deforming metals. The uniaxial and shear results are verified via the von Mises criterion while the biaxial results are verified by comparison to experimental results from the literature. The model which is being considered, although nonlinear, is relatively simple in that only two evolutionary equations are required to model inelastic strain and backstress at a material point. Thus the model being presented utilized only on internal variable, i.e. the backstress. Rate dependent characteristics are evaluated both analytically and numerically and show that the model being considered here is rate independent.

NOTE

The present report and the previous technical report NCEER-89-0018 (*Multidimensional Models of Hysteretic Material Behavior for Vibration Analysis of Shape Memory Energy Absorbing Devices*, by E.J. Graesser and F.A. Cozzarelli) are based on separate topics given in the Ph.D. dissertation by E.J. Graesser (see [3]). Report NCEER-89-0018 was concerned with a theoretical development of a constitutive law for shape memory alloys (SMA), which absorb energy by phase transformation. A paper entitled *Shape Memory Alloys as New Materials for Aseismic Isolation* by E.J. Graesser and F.A. Cozzarelli, has also been accepted for publication in the **ASCE Journal of Engineering Mechanics**. This paper includes the one-dimensional work on SMA given in NCEER-89-0018, plus later experimental work done in the NCEER laboratory and reported in the dissertation. The present report is concerned with a new multidimensional constitutive model for plastically deforming metals, and includes a comparison with hysteretic data given in the literature. The material in this report will also be presented at the conference "High Temperature Constitutive Modeling; Theory and Application," to be held at the 1991 ASME Winder Annual Meeting in Atlanta, Georgia.

ACKNOWLEDGEMENT

The research presented in this paper was supported by the National Center for Earthquake Engineering Research (NCEER) under NSF Master Contract No. ECE-86-07591. This support is gratefully acknowledged. The authors also wish to acknowledge Dr. S. Duffy for his helpful discussion on viscoplasticity and for his generous supply of technical articles on the subject.

TABLE OF CONTENTS

LIST OF ILLUSTRATIONS

SECTION 1
INTRODUCTION

Structural systems subjected to seismically induced vibration can now be protected by using passive control measures such as base isolation and added structural dampers [1,2]. Successful studies made on elastomeric, lead-rubber, and frictional base isolation devices have ultimately led to implementation of base isolation technology in a variety of worldwide locations. During seismic activity, the flexibility and energy absorbing characteristics of these devices isolate the building from damaging horizontal ground motion. The isolation devices which are employed in these techniques typically undergo cyclic deformation well into the inelastic range and thus exhibit hysteretic behavior.

In order to explore a variety of phenomena associated with hysteretic deformation of energy absorbing devices, a general material model was developed [3] based on Ozdemir's form [4] of the Bonc-Wen one-dimensional hysteretic model [5]. Ozdemir's model has many features which render it useful. It was originally developed so that the force-deformation characteristics of base isolation energy absorbing devices could be predicted computationally. Also, it can be used to model rate-independent behavior, which is useful since many isolation devices are only slightly sensitive to the applied rate of loading [4,6]. In addition, the equations of the model contain constants that are physically motivated. Furthermore, Ozdemir's model expresses the strain rate as the sum of elastic and inelastic components with the inelastic component being a function of overstress, and as such is similar to established models of unified creep and viscoplasticity [7,8].

Because the applied technologies associated with the base isolation concept and the concept of added dampers are relatively new, analytical investigations involving energy absorbing devices have used one-dimensional models of hysteresis [9,10,6]. Therefore, in order to include multi-axial loading conditions, the one-dimensional model of Ozdemir was extrapolated to three- dimensions following a manner originally developed by Prager [11], and more recently adapted to a power law for steady creep behavior [12]. The resulting three-dimensional model will be useful for analysis and design of potential energy absorbing devices in structural damping applications. Finally, the model is considered form a thermodynamic standpoint in the appendix.

SECTION 2
OZDEMIR'S MODEL FOR HYSTERETIC BEHAVIOR

Characterization of hysteretic material behavior is accomplished here by extending a rate independent model for hysteretic behavior due to Ozdemir [4]. Constantinou [13] showed that Ozedmir's model is a special case of the Bonc-Wen model [5]; also see [14]. The equations which describe Ozdemir's model are as follows:

$$\dot{\sigma} = E\left[\dot{\varepsilon} - |\dot{\varepsilon}|\left(\frac{\sigma-\beta}{Y}\right)^n\right] \tag{2.1}$$

$$\dot{\beta} = \alpha E\,|\dot{\varepsilon}|\left(\frac{\sigma-\beta}{Y}\right)^n \tag{2.2}$$

where:

- σ = One dimensional stress.
- ε = One dimensional strain.
- β = One dimensional backstress.
- E = Elastic modulus.
- Y = Yield stress.
- α = Constant controlling the slope of the σ - ε curve. Given by $\alpha = E_y/(E-E_y)$ where E_y is the slope of the σ - ε curve after yielding.
- n = Constant controlling the sharpness of transition from elastic to plastic states.
- $(\dot{})$ = Ordinary time derivative.

Note from Eq. (2.2) that the function β is an evolving internal stress variable called backstress and the difference σ-β is analogous to the overstress (or effective stress) used in many viscoplastic laws [7,8].

By rearranging Eq. (2.1) it follows that:

$$\dot{\varepsilon} = \frac{\dot{\sigma}}{E} + |\dot{\varepsilon}|\left(\frac{\sigma-\beta}{Y}\right)^n$$

Examination of this equation reveals that the total strain is made up of two separate components 1) a linear elastic component σ/E and 2) a nonlinear inelastic component, ε^{in}, which is described by the rate expression $\dot{\varepsilon}^{in} = |\dot{\varepsilon}|\,[(\sigma-\beta)/Y]^n$. This inelastic component is a function of the strain rate $\dot{\varepsilon}$ and the overstress σ-β. This model, although nonlinear, is relatively simple in that there is only one internal variable, namely the backstress β.

We will now show that for this model the stress and strain are independent of the applied rates of loading, i.e. they are not dependent on either of the rates $\dot{\sigma}$ or $\dot{\varepsilon}$. The case of positive strain rate loading is used. By subtracting Eq. (2.2) from Eq. (2.1) the following differential equation is obtained:

$$\dot{\sigma} - \dot{\beta} = E\dot{\varepsilon}\left[1 - (1+\alpha)\left(\frac{\sigma-\beta}{Y}\right)^n\right]$$

This result can be re-expressed as:

$$d\varepsilon = \frac{1}{E}\,\frac{d(\sigma-\beta)}{1 - (1+\alpha)\left(\frac{\sigma-\beta}{Y}\right)^n}$$

Then by integration, the solution for the strain can be shown to be

$$\varepsilon = \frac{Y}{E(1+\alpha)^{1/n}}\int_0^{\frac{\sigma-\beta}{Y}} \frac{d\varepsilon}{1-\xi^n}$$

It can easily be seen that the above integral is a function only of the overstress $\sigma-\beta$, i.e., $\varepsilon = \phi(\sigma-\beta)$. By this process it is clear that Eqs. (2.1) and (2.2) represent rate independent stress-strain behavior. For the special case where n=1, the following result can be readily obtained:

$$\sigma = \frac{E\alpha}{1+\alpha}\,\varepsilon + \frac{Y}{(1+\alpha)^2}\left[1 - \exp\left\{-\frac{E(1+\alpha)}{Y}\,\varepsilon\right\}\right]$$

This result shows the explicit nature of the rate independence.

Before proceeding further, let us first take a moment to examine the inelastic contribution to the strain rate more carefully:

$$\dot{\varepsilon}^{in} = |\dot{\varepsilon}|\left(\frac{\sigma-\beta}{Y}\right)^n \tag{2.3}$$

This expression is very similar in form to the following rate sensitive flow rule for the nonlinear Kelvin-St. Venant (K-V) viscoplastic model:

$$\dot{\varepsilon}^{p} = \begin{cases} 0 & \text{for} \quad \sigma < Y \\ \dfrac{1}{t_\varepsilon}\left(\dfrac{\sigma-Y}{\mu}\right)^n & \text{for} \quad \sigma \geq Y \end{cases} \tag{2.4}$$

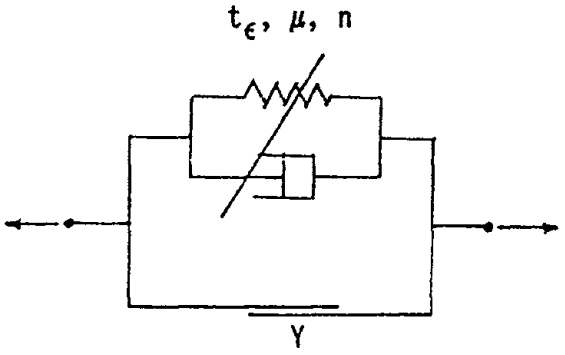

Kelvin-St. Venant

Viscoplastic Model

For the flow rule of the K-V model $\dot{\varepsilon}^p$ is the plastic strain rate (or viscoplastic flow rate), and t_ε, μ, and n are material constants. The K-V model incorporates a specific condition for yielding (i.e. σ=Y) which, when met, permits plastic deformation of the nonlinear power law type. There are both similarities and differences which are observed when comparing Eqs. (2.3) and (2.4). Both equations are similar in that they are nonlinear power laws for the evolution of inelastic strain with time. In both cases a stress difference (or overstress) is raised to a power n. Also, both give hardening behavior in the inelastic regime.

However, major differences also exist between Eqs. (2.3) and (2.4). The first difference lies in the use of the variable backstress β in Eq. (2.3) versus a specific yield condition in Eq. (2.4) (i.e. σ=Y). The internal backstress is a continually evolving function which is small for stress levels below the yield stress. As the stress increases, the difference σ-β becomes significant and leads to increased growth of inelastic strain. In this way the internal variable of backstress introduces work hardening and is a generalization of kinematic hardening of classical plasticity [4]. The other aspect which separates Eq. (2.3) from (2.4) is the leading factor in the right hand side of each equation. In Eq. (2.4) the leading factor is $1/t_\varepsilon$ where t_ε is a constant relaxation time of the K-V element. In Eq. (2.3) the factor $|\dot{\varepsilon}|$ is used. This quantity is the absolute value of the total strain rate ($\dot{\varepsilon}^{el}+\dot{\varepsilon}^{in}$) and is an input quantity which changes with time. Thus Eq. (2.3) describes the time rate of change of inelastic strain as dependent not only upon the state of stress, but also upon the rate of application of the total strain. It is this aspect of the form of Eq. (2.3) that causes Ozdemir's model to exhibit rate independent behavior. We will now show that while Eqs. (2.1) and (2.2) do not contain an apparent yield condition, their use does give a well defined yield point. This will be shown by using the results of selected computational analyses.

Given a set of material data (E,Y,α,n) and a sinusoidal history of strain as input, a FORTRAN algorithm was used to solve Eqs. (2.1) and (2.2) numerically. Fourth order Runge-Kutta forward integration was used in conjunction with small time steps and double precision

accuracy. The initial uniaxial material properties for A-36 structural steel [15] were used in computations; these properties are as follows:

Material Data for A-36

Materials Property	**Symbol**	**Value**
Young's modulus	E	28500 ksi
Axial initial Yield stress	Y	30 ksi
Plastic modulus	E_y	550 ksi

Using the definition of α given following Eq. (2.2) $\alpha = .0197$.

Using this data, homogeneous initial conditions, and $\varepsilon = .016 \sin \omega t$, Eqs. (2.1) and (2.2) were integrated numerically; and numerous results for the stress-strain material behavior were plotted graphically [3]. More concise results will be presented here. Figure 2-1 gives the calculated response for an overstress power of n=15. Also shown is a dashed curve that represents the transition from elastic to inelastic behavior at the lower bound of n=1. For n=1 the loop is well rounded and the transition from elastic to inelastic behavior is smooth; as n increases in value, the transition from elastic to plastic behavior becomes much sharper as shown for the case of n=15. In fact this case nearly replicates elastic-plastic material behavior with linear work hardening (also called bilinear behavior).

Since the transition from elastic to plastic material behavior is very sharp when n=15, it is possible to check the initial yield point as given by the model. Examination of Figure 2-1 reveals that the proportional limit of the initial loading branch reproduces the actual material yield for A-36 steel, i.e. Y=30 ksi. Thus the actual material yield point is well represented by the model. Also, it can be seen from that the Baushinger effect is manifested with the model. Thus, two important physical features of plastic material behavior are reproduced by Eqs. (2.1) and (2.2) namely the material yield point and the Bauschinger effect.

The model is also able to properly reproduce the slope of both the elastic and plastic portions of the stress strain curves, i.e. E and E_y. This is shown in Figure 2-2 for n=15. In this figure the slope of the hysteresic stress-strain curve of Figure 2-1 is plotted. The slope can be determined exactly by dividing Eq. (1) by $\dot{\varepsilon}$ thus giving:

$$\frac{d\sigma}{d\varepsilon} = E\left[1 - \mathrm{sgn}(\dot{\varepsilon})\left|\frac{\sigma-\beta}{Y}\right|^{n-1}\left(\frac{\sigma-\beta}{Y}\right)\right]$$

The results given in Figure 2-2 show that the elastic slope E is correctly reproduced by the model, i.e. E = 28500 ksi. The value of the plastic slope, E_y, cannot be easily read off the plot. However, a check of the data from the numerical calculations gave the plastic slope as 550.6 ksi, a very small departure from the actual material value of E_y = 550 ksi. Thus the values of the

elastic and plastic moduli are well represented by the Ozdemir's hysteretic model. It is therefore possible to characterize one-dimensional hysteretic material behavior easily and accurately using Eqs. (2.1) and (2.2).

$\varepsilon = A \sin \omega t$

Y = 30 ksi $\nu = 0.5$

E = 28500 ksi

$\alpha = 0.0197$ n = 15 (--- n = 1)

$\omega = 1$ A = .016

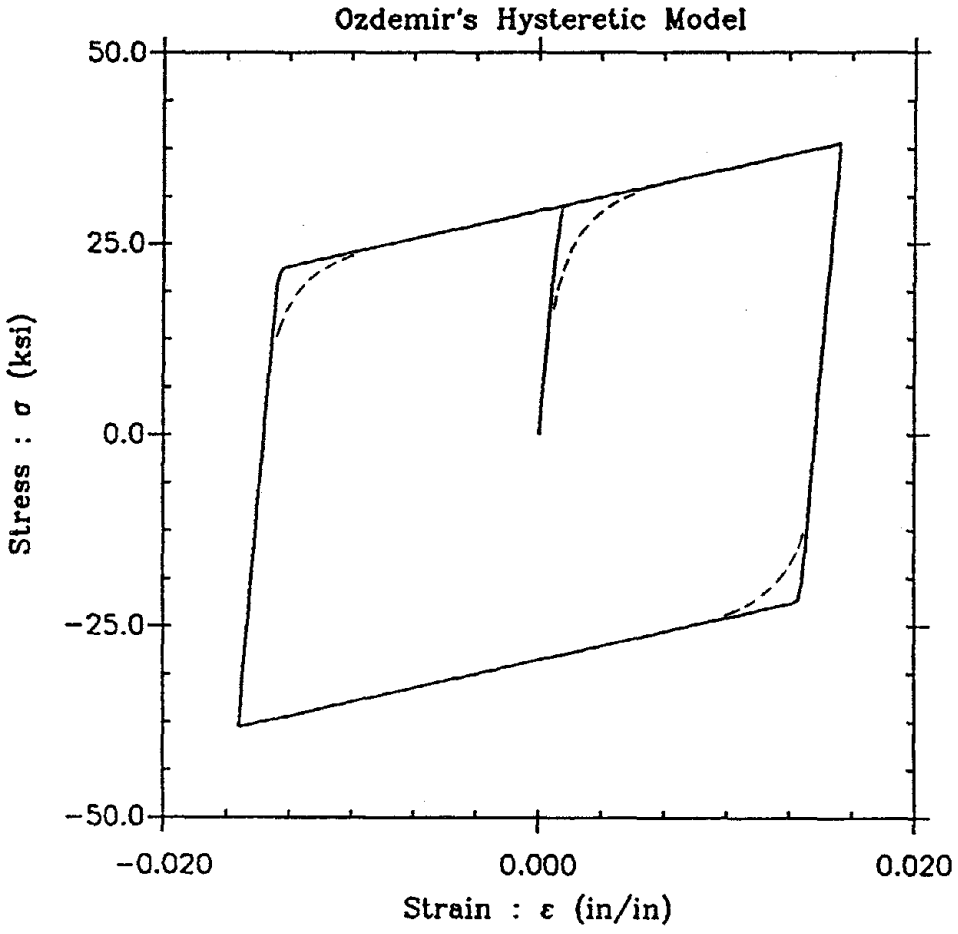

Figure 2-1 Hysteresis with n = 15, Bilinear Behavior (dashed line: n=1).

$\varepsilon = A \sin \omega t$

$Y = 30$ ksi $\quad \nu = 0.5$

$E = 28500$ ksi

$\alpha = 0.0197 \quad n = 15$

$\omega = 1 \quad A = .016$

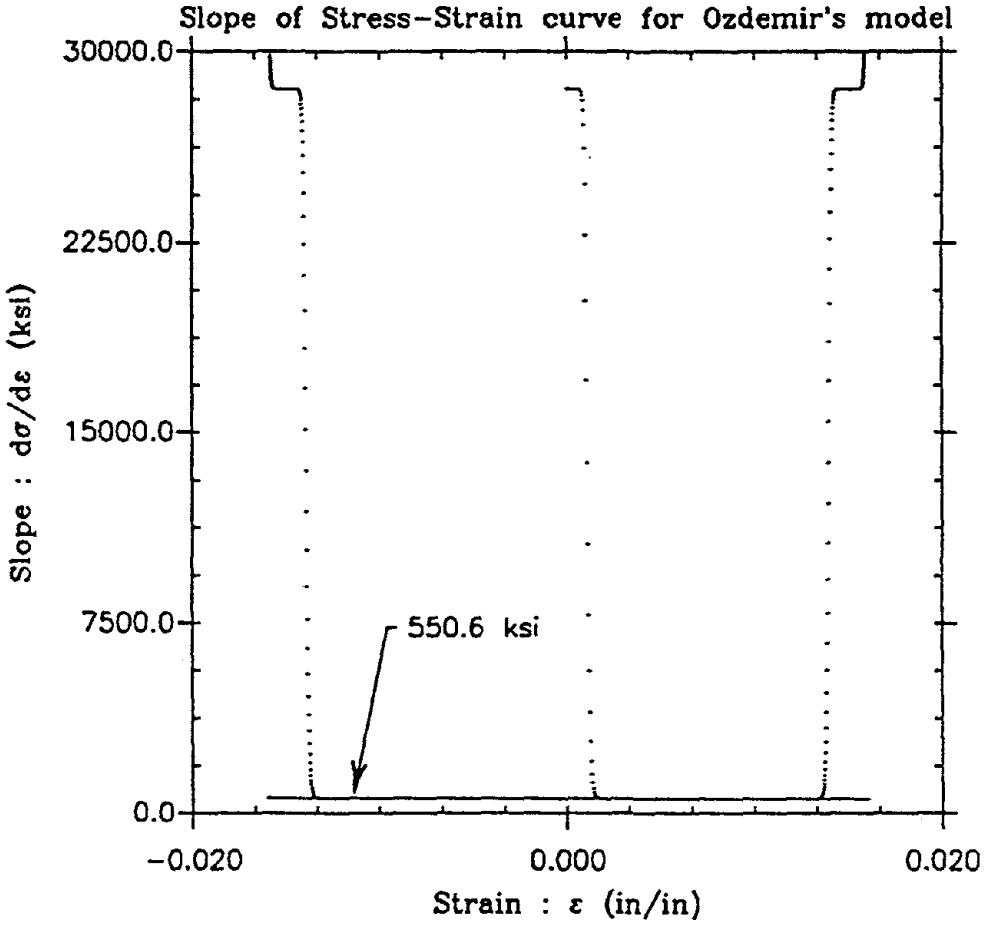

Figure 2-2 Slope of Hysteresis Loop with n = 15.

SECTION 3
EXTENSION OF OZDEMIR'S MODEL TO A THREE-DIMENSIONAL LAW OF PLASTICITY

To begin, Eqs. (2.1) and (2.2) are rewritten specifically for the axial loading direction:

$$\dot{\varepsilon}_{11} = \frac{\dot{\sigma}_{11}}{E} + \left|\dot{\varepsilon}_{11}\right| \left(\frac{\sigma_{11} - \beta_{11}}{Y}\right)^n \tag{3.1}$$

$$\dot{\beta}_{11} = E\alpha \left|\dot{\varepsilon}_{11}\right| \left(\frac{\sigma_{11} - \beta_{11}}{Y}\right)^n \tag{3.2}$$

The subscripts 11 represent the x direction of a Cartesian coordinate system. Recall that n is restricted to odd positive integers. If one wishes to work with this law and have more freedom in the choice of the power n, then Eqs. (3.1) and (3.2) can be re-expressed in another equivalent form (e.g. see [16]) as follows:

$$\dot{\varepsilon}_{11} = \frac{\dot{\sigma}_{11}}{E} + \left|\dot{\varepsilon}_{11}\right| \left(\frac{\sigma_{11} - \beta_{11}}{Y}\right)^{n-1} \left(\frac{\sigma_{11} - \beta_{11}}{Y}\right) \tag{3.3}$$

$$\dot{\beta}_{11} = E\alpha \left|\dot{\varepsilon}_{11}\right| \left(\frac{\sigma_{11} - \beta_{11}}{Y}\right)^{n-1} \left(\frac{\sigma_{11} - \beta_{11}}{Y}\right) \tag{3.4}$$

The only restriction now remaining on n is that it have values such that $n \geq 1$. For now however, we will proceed using Eqs. (3.1) and (3.2).

In Shames and Cozzarelli [12] a procedure for extending one dimensional power laws to a three dimensional tensor expression is presented for the case of steady creep. The extension of Eqs. (3.1) and (3.2) to three dimensions will follow this procedure since the rate expressions are of the power law type. Considering Eq. (3.1), the first term on the right hand side is the elastic part of the strain rate and second term is the nonlinear inelastic part of the strain rate. In the extension of Eq. (3.1) the three dimensional counterpart to the elastic component of the one dimensional strain follows directly from the theory of elasticity, i.e.

$$\varepsilon_{ij}^{el} = \frac{1+\upsilon}{E}\sigma_{ij} - \frac{\upsilon}{E}\sigma_{kk}\,\delta_{ij}$$

where ε_{ij}^{el} is the elastic component of the total strain tensor, σ_{ij} is the stress tensor, E is Young's modulus, υ is the elastic Poisson ratio, and δ_{ij} is the Kronecker delta.

In extending the inelastic component of the uniaxial strain rate to three dimensions, we begin with the following:

$$\dot{\varepsilon}_{11}^{in} = |\dot{\varepsilon}_{11}| \left(\frac{\sigma_{11} - \beta_{11}}{Y} \right)^n \tag{3.5}$$

Inelastic (or plastic) deformation is taken to arise from dislocation glide on slip planes. Since only small interatomic distances are involved in this process of consecutive slip, no volume change is associated with this effect and the material behavior is taken as incompressible. Therefore the inelastic strain must be a deviatoric quantity in three dimensions. Thus, Eq. (3.5) will be rewritten in terms of associated deviator tensors. Recall that the deviator tensor is defined as follows:

$$\text{Deviator Tensor:} \quad z_{ij} = \zeta_{ij} - \frac{\zeta_{kk}}{3} \delta_{ij} \quad , \quad z_{kk} = 0$$

Here ζ_{ij} is a general tensor quantity and z_{ij} is its deviatoric counterpart.

For the case of one-dimensional loading the stress, stress deviator, backstress, and backstress deviator tensors are as follows:

$$\sigma_{ij} = \begin{bmatrix} \sigma_{11} & 0 & 0 \\ 0 & 0 & 0 \\ 0 & 0 & 0 \end{bmatrix} \qquad s_{ij} = \begin{bmatrix} \frac{2}{3}\sigma_{11} & 0 & 0 \\ 0 & -\frac{1}{3}\sigma_{11} & 0 \\ 0 & 0 & -\frac{1}{3}\sigma_{11} \end{bmatrix}$$

$$\beta_{ij} = \begin{bmatrix} \beta_{11} & 0 & 0 \\ 0 & 0 & 0 \\ 0 & 0 & 0 \end{bmatrix} \qquad b_{ij} = \begin{bmatrix} \frac{2}{3}\beta_{11} & 0 & 0 \\ 0 & -\frac{1}{3}\beta_{11} & 0 \\ 0 & 0 & -\frac{1}{3}\beta_{11} \end{bmatrix}$$

The tensors of inelastic strain and total strain rate are:

$$\varepsilon_{ij}^{in} = \begin{bmatrix} \varepsilon_{11} & 0 & 0 \\ 0 & -\frac{1}{2}\varepsilon_{11} & 0 \\ 0 & 0 & -\frac{1}{2}\varepsilon_{11} \end{bmatrix} \qquad \dot{\varepsilon}_{ij} = \begin{bmatrix} \dot{\varepsilon}_{11} & 0 & 0 \\ 0 & -\gamma\dot{\varepsilon}_{11} & 0 \\ 0 & 0 & -\gamma\dot{\varepsilon}_{11} \end{bmatrix}$$

Note that the Poisson ratio associated with inelastic behavior is 1/2. This gives the necessary deviatoric behavior associated with the incompressible inelastic material response. The total strain rate does not have a constant Poisson ratio however. The Poisson ratio associ-

ated with the total strain rate is denoted here as γ. The ratio γ becomes variable in the transition from elastic to inelastic behavior and can be shown to be as follows for the uniaxial case:

$$\gamma = \frac{1}{2} - \frac{1}{E}\left(\frac{1}{2} - \upsilon\right)\frac{d\sigma_{11}}{d\varepsilon_{11}}$$

From this it is easy to see that during elastic loading $\gamma=\upsilon$ and during inelastic loading $\gamma\approx.5$. Since the slope associated with inelastic behavior is usually much smaller in magnitude than the modulus associated with purely elastic behavior, it is reasonable to assume that $\gamma = 1/2$ in the extension of the total strain rate of Eq. (3.5) to 3D. Therefore the tensor of total strain rate is approximately equal to its deviatoric counterpart e_{ij}, i.e.

$$\dot{\varepsilon}_{ij} \approx \dot{e}_{ij} \qquad \text{(during inelastic loading)} \tag{3.6}$$

Thus when Eq. (3.5) is rewritten in terms of the uniaxial components of associated deviatoric tensors and when the assumption of Eq. (3.6) is also employed, we obtain the following result:

$$\dot{\varepsilon}_{11}^{in} = A\left|\dot{e}_{11}\right|\Sigma_{11}^{\,n} \tag{3.7}$$

where:

$$A = \left(\frac{3}{2Y}\right)^n \qquad , \ \Sigma_{11} = s_{11} - b_{11}$$

The difference s_{11}-b_{11} is referred to here as the effective stress and denoted as Σ_{11}. The term overstress may also be used in conjunction with this expression.

It is now of interest to examine the three dimensional counterparts of the one dimensional quantities in Eq. (3.7) and we will proceed in the manner of Prager [11].

1D Quantity	**3D Counterpart**
ε_{11}^{in}	ε_{ij}^{in} (deviatoric)
Σ_{11}	Σ_{ij} (deviatoric)
$\left\|\dot{e}_{11}\right\|$	?
$\Sigma_{11}^{\,n}$	?

The three dimensional forms of the last two quantities are most easily determined by using matrix notation. In matrix notation (denoted by underscore _) we have the following one to one correspondences (indicated by ~)

$$\varepsilon_{ij}^{in} \sim \underline{E}^{in} \qquad\qquad \dot{\varepsilon}_{ij}^{in} \sim \underline{\dot{E}}^{in}$$

$$e_{ij} \sim \underline{E} \qquad\qquad \dot{e}_{ij} \sim \underline{\dot{E}} \qquad\qquad \Sigma_{ij} \sim \underline{S}$$

Using matrix notation, the three dimensional counterparts of $\Sigma_{11}{}^n$ and $|\dot{e}_{11}|$ are as follows:

$$\Sigma_{11}{}^n \quad \longleftrightarrow \quad \underline{S}^n$$

$$|\dot{e}_{11}| \quad \longleftrightarrow \quad \sqrt{\frac{2}{3}}\sqrt{\underline{\dot{E}} : \underline{\dot{E}}}$$

The quantity $\underline{S}^n$ is the matrix of effective stresses raised to the power n and has the following correspondence to the effective stress tensor:

$$\underline{S}^n \sim \Sigma_{ij}\,\Sigma_{jk}\,\Sigma_{kl} \ldots \Sigma_{pq}\,\Sigma_{qr} \qquad \text{(n factors)}$$

The quantity $\underline{\dot{E}}:\underline{\dot{E}}$ $(\sim \dot{e}_{ij}\,\dot{e}_{ij})$ is the scalar product of the matrix $\underline{\dot{E}}$. Note that the square root specified above is to be taken as positive. It should also be noted that the three dimensional quantity $\sqrt{2/3}\sqrt{\underline{\dot{E}} : \underline{\dot{E}}}$ will reduce to its proper one dimensional counterpart in the case of the uniaxial test applied to an incompressible material. Also this three dimensional quantity is analogous to the effective plastic strain rate used in the plasticity theory [12].

Using the properties of powers of tensors, the matrix quantity $\underline{S}^n$ can be expressed in a more useful and compact form by making use of the Caley-Hamilton theorem. Specifically:

$$\underline{S}^n = p(J_2,J_3)\underline{S}^2 + q(J_2,J_3)\underline{S} + r(J_2,J_3)\underline{I} \tag{3.8}$$

Here J_2 and J_3 are the second and third invariants of the effective stress tensor which are defined as follows:

$$J_2 = \frac{1}{2}\,\Sigma_{ij}\Sigma_{ij} \qquad , \qquad J_3 = \frac{1}{3}\,\Sigma_{ij}\Sigma_{jk}\Sigma_{ki}$$

The quantities $p(J_2,J_3)$, $q(J_2,J_3)$, and $r(J_2,J_3)$ are polynomials of the invariants J_2 and J_3 and these polynomials can be determined via the Caley-Hamilton theorem:

$$\underline{S}^3 = J_2\,\underline{S} + J_3\,\underline{I}$$

Therefore the one dimensional model of Eq. (3.7) can now be extended, term by term, to a direct three dimensional counterpart:

1D Model:

$$\dot{\varepsilon}_{11}^{in} = A|\dot{e}_{11}|\Sigma_{11}^{n}$$

3D Direct Extension:

$$\underline{\dot{E}}^{in} = A\sqrt{\frac{2}{3}}\sqrt{\underline{\dot{E}}:\underline{\dot{E}}}\,\underline{S}^{n} \tag{3.9}$$

Now, recall that the trace of the inelastic strain rate tensor must vanish due to the incompressibility assumption. Therefore, according to Eq. (3.9) $\mathrm{tr}\underline{S}^{n}= 0$ thus requiring that:

$$-2J_2 p(J_2,J_3) = 3r(J_2,J_3) \tag{3.10}$$

However this relationship results in a contradiction because the equality does not hold for general values of the exponent n.

To alleviate the inconsistency caused by Eq. (3.10) we introduce the coefficients α, β, and ξ into the terms of $\underline{S}^{n}$ in Eq. (3.8) thereby producing the following new relationship for the inelastic strain rate:

$$\underline{\dot{E}}^{in} = A\sqrt{\frac{2}{3}}\sqrt{\underline{\dot{E}}:\underline{\dot{E}}}\left[\alpha\, p(J_2,J_3)\ \underline{S}^2 + \beta\, q(J_2,J_3)\ \underline{S} + \xi\, r(J_2,J_3)\ \underline{I}\right]$$

Now upon taking the trace of $\underline{E}^{in}$ a relationship between ξ and α is produced:

$$\mathrm{tr}\underline{\dot{E}} = 0 \longrightarrow \xi = -\frac{p(J_2,J_3)\ \mathrm{tr}\underline{S}^2}{3r(J_2,J_3)}\,\alpha$$

Thus the proposed 3D extension becomes:

$$\underline{\dot{E}}^{in} = A\sqrt{\frac{2}{3}}\sqrt{\underline{\dot{E}}:\underline{\dot{E}}}\left[C\, q(J_2,J_3)\ \underline{S} + D\, p(J_2,J_3)\left(\underline{S}^2 - \frac{1}{3}\mathrm{tr}\underline{S}^2\ \underline{I}\right)\right] \tag{3.11}$$

Note that the quantity $\underline{S}^2 - 1/3\mathrm{tr}\underline{S}^2\ \underline{I}$ is the deviator of the matrix $\underline{S}^2$. Also the coefficients A, α, and β are combined such that $C=A\alpha$ and $D=A\beta$.

We are now at a point where we can revert back to index notation. The following list will show the proper correspondences between matrix and index notation:

Matrix Notation	Index Notation
$\dot{\underline{E}}^{in}$	$\dot{\varepsilon}_{ij}^{in}$
$\underline{S}$	Σ_{ij}
$\dot{\underline{E}}:\dot{\underline{E}}$	$\dot{e}_{ij}\dot{e}_{ij}$
$\underline{S}^2 - (1/3)\mathrm{tr}\underline{S}^2\underline{I}$	$\Sigma_{ij}\Sigma_{kj} - (1/3)\Sigma_{lm}\Sigma_{lm}\delta_{ij}$

By defining the following quantities:

$$K_2 = \frac{1}{2} e_{ij} e_{ij} \qquad \text{(2nd Invariant of the total strain rate deviation)}$$

$$R_{ij} = \Sigma_{ij}\Sigma_{kj} - \frac{1}{3}\Sigma_{lm}\Sigma_{lm}\delta_{ij}$$

Eq. (3.9) takes on the following form in index notation:

$$\dot{\varepsilon}_{ij}^{in} = \frac{2}{3}\sqrt{3K_2}\,[C\,q(J_2,J_3)\,\Sigma_{ij} + D\,p(J_2,J_3)\,R_{ij}] \tag{3.12}$$

Thus Eq. (3.12) is a general three dimensional form of Eq. (3.5). We can gain more insight into the nature of Eq. (3.12) by utilizing the following properties of J_2 and J_3:

$$\frac{\partial J_2}{\partial \sigma_{ij}} = \Sigma_{ij} \qquad \frac{\partial J_3}{\partial \sigma_{ij}} = R_{ij}$$

And we can introduce a potential function $\phi(J_2,J_3)$ such that:

$$\frac{\partial \phi}{\partial J_2} = C\,q(J_2,J_3) \qquad \frac{\partial \phi}{\partial J_3} = D\,p(J_2,J_3)$$

Doing this and utilizing the chain rule Eq. (3.12) can be rewritten as:

$$\dot{\varepsilon}_{ij}^{in} = \frac{2}{3}\sqrt{3K_2}\,\frac{\partial \phi(J_2,J_3)}{\partial \sigma_{ij}} \tag{3.13}$$

Note that the function ϕ incorporates not only the stress but also the internal backstress (via the effective stress Σ_{ij} contained in J_2 and J_3). Thus the use of the effective stress in ϕ allows for a definition of a surface in stress space which is analogous to the yield surfaces of classical plasticity which include kinematic hardening rules.

For most applications involving plastically deforming materials the inelastic response depends only on the invariant J_2 [12] (an example of such a case is the Lévy-Mises flow rule). For such cases, we can simplify Eq. (3.13) as follows:

$$\dot{\varepsilon}_{ij}^{in} = \frac{2}{3}\sqrt{3K_2}\,\frac{\partial\phi(J_2)}{\partial\sigma_{ij}} = \frac{2}{3}\sqrt{3K_2}\,C\,q(J_2)\,\Sigma_{ij}$$

It is clear from this result that the inelastic strain rate points in the same direction as the effective stress, outward from the surface ϕ. The magnitude of $\dot{\varepsilon}_{ij}^{in}$ is determined not only by the state of stress, but also by the magnitude of the total strain rate, $\dot{\varepsilon}_{ij}$. This is due to the presence of K_2.

For odd powers of n it can be shown [12] that $q(J_2) = J_2^{(n-1)/2}$. Thus:

$$\dot{\varepsilon}_{ij}^{in} = C\frac{2}{3}\sqrt{3K_2}\,J_2^{\frac{n-1}{2}}\,\Sigma_{ij} \tag{3.14}$$

By defining the constant C as $C = (3/2Y)\,(\sqrt{3}/Y)^{n-1}$ the extrapolated result given by Eq. (3.14) will properly reduce to the one dimensional material law Eq. (3.5). Also this choice of C corresponds to the use of a von Mises type yield criterion as seen in the following result:

$$\dot{\varepsilon}_{ij}^{in} = \sqrt{3K_2}\left[\frac{J_2}{Y^2/3}\right]^{\frac{n-1}{2}}\frac{\Sigma_{ij}}{Y} \tag{3.15}$$

where quantity $J_2/(Y^2/3)$ is analogous to the von Mises yield criterion.

To complete the details of the extrapolation procedure let us define a dimensionless counterpart to the invariant J_2 as follows:

$$J_2^0 = \frac{1}{2}\,\frac{\Sigma_{ij}}{Y}\,\frac{\Sigma_{ij}}{Y}$$

Also, recalling that $\Sigma_{ij} = s_{ij} - b_{ij}$ we finally produce the following result:

$$\dot{\varepsilon}_{ij}^{in} = \sqrt{3K_2}\,\left[3J_2^0\right]^{\frac{n-1}{2}}\left[\frac{s_{ij} - b_{ij}}{Y}\right] \tag{3.16}$$

The net effect of the extrapolation results in the following simple steps:

$$\varepsilon_{11}^{el} \rightarrow \varepsilon_{ij}^{el}$$

$$\left| \frac{3}{2}\dot{e}_{11} \right| \rightarrow (3K_2)^{1/2}$$

$$\varepsilon_{11}^{in} \rightarrow \varepsilon_{ij}^{in}$$

$$s_{11} \rightarrow s_{ij}$$

$$\left| \frac{(3/2)\,(s_{11} - b_{11})}{Y} \right| \rightarrow \left(3J_2^0\right)^{1/2}$$

$$b_{11} \rightarrow b_{ij}$$

Note that quantities operated on by the absolute value are extended to the positive square root of their associated invariant. Thus the constitutive relation for the total strain rate tensor composed of linear elastic and nonlinear inelastic parts is as follows:

$$\dot{\varepsilon}_{ij} = \frac{1+\upsilon}{E}\dot{\sigma}_{ij} - \frac{\upsilon}{E}\dot{\sigma}_{kk}\delta_{ij} + (3K_2)^{1/2}(3J_2^0)^{\frac{n-1}{2}}\left[\frac{s_{ij} - b_{ij}}{Y}\right] \tag{3.17}$$

Next, the expression that defines the evolution of the backstress (Eq. (3.2)) also needs to be extended to three dimensions. Eq. (3.2) is first recast into an equivalent expression which is deduced by considering Eqs. (3.1) and (3.2) together. The specific form of the recast equation is:

$$\dot{\beta}_{11} = E\alpha\left[\dot{\varepsilon}_{11} - \frac{\dot{\sigma}_{11}}{E}\right]$$

It is then immediately evident that:

$$\dot{\beta}_{11} = E\alpha\,\dot{\varepsilon}_{11}^{in}$$

which, when re-expressed in terms of the deviator expressions of the uniaxial test, becomes:

$$\dot{b}_{11} = \frac{2}{3}\,E\alpha\dot{\varepsilon}_{11}^{in}$$

In the extension to three dimensions $\dot{b}_{11}$ becomes $\dot{b}_{ij}$ and $\dot{\varepsilon}_{11}^{in}$ becomes $\dot{\varepsilon}_{ij}^{in}$ which produces the following result:

$$\dot{b}_{ij} = \frac{2}{3}\,E\alpha\,(3K_2)^{1/2}(3J_2^0)^{\frac{n-1}{2}}\left(\frac{s_{ij} - b_{ij}}{Y}\right) \tag{3.18}$$

Therefore, the fully extended formulation expressed in terms of the strain rate tensor is given by Eqs. (3.17) and (3.18). This proposed law of metal plasticity is now rewritten for clarity:

$$\dot{\varepsilon}_{ij} = \frac{1+\upsilon}{E}\dot{\sigma}_{ij} - \frac{\upsilon}{E}\dot{\sigma}_{kk}\delta_{ij} + (3K_2)^{1/2}(3J_2^0)^{\frac{n-1}{2}}\left[\frac{s_{ij} - b_{ij}}{Y}\right] \tag{3.19}$$

$$b_{ij} = \frac{2}{3}E\alpha\,(3K_2)^{1/2}(3J_2^0)^{\frac{n-1}{2}}\left(\frac{s_{ij} - b_{ij}}{Y}\right) \tag{3.20}$$

where:

$$s_{ij} = \sigma_{ij} - \frac{1}{3}\sigma_{kk}\delta_{ij} \qquad e_{ij} = \varepsilon_{ij} - \frac{1}{3}\varepsilon_{kk}\delta_{ij}$$

$$b_{ij} = \beta_{ij} - \frac{1}{3}\beta_{kk}\delta_{ij} \qquad K_2 = \frac{1}{2}\dot{e}_{ij}\dot{e}_{ij}$$

$$J_2^0 = \frac{1}{2}\left(\frac{s_{ij} - b_{ij}}{Y}\right)\left(\frac{s_{ij} - b_{ij}}{Y}\right)$$

Now, let the formulation of Eqs. (3.19) and (3.20) be examined for the special case of uniaxial behavior. In this examination the changes in volume which result from the Poisson effect will be included.

It can be shown that γ is as follows for this uniaxial case. By carrying out the necessary mathematical manipulations and simplifications, we have:

$$(3K_2)^{1/2} = (1+\gamma)\left|\dot{\varepsilon}_{11}\right|$$

$$(3J_2^0)^{\frac{n-1}{2}} = \left|\frac{\sigma_{11} - \beta_{11}}{Y}\right|$$

$$\gamma = \frac{\upsilon+1}{1 - \frac{2}{3}\left[\frac{1}{2} - \upsilon\right]\left[\mathrm{sgn}(\dot{\varepsilon}_{11})\left|\frac{\sigma_{11} - \beta_{11}}{Y}\right|^{n-1}\left(\frac{\sigma_{11} - \beta_{11}}{Y}\right)\right]} - 1 \tag{3.21}$$

Thus the uniaxial components of Eqs. (3.19) and (3.20) are as follows:

$$\dot{\varepsilon}_{11} = \frac{\dot{\sigma}_{11}}{E} + \frac{2}{3}(1+\gamma)\left|\dot{\varepsilon}_{11}\right|\left|\frac{\alpha_{11} - \beta_{11}}{Y}\right|^{n-1}\left(\frac{\sigma_{11} - \beta_{11}}{Y}\right) \tag{3.22}$$

$$\dot{\beta}_{11} = \frac{2}{3} E\alpha(1+\gamma) \left| \dot{\varepsilon}_{11} \right| \left| \frac{\alpha_{11} - \beta_{11}}{Y} \right|^{n-1} \left(\frac{\sigma_{11} - \beta_{11}}{Y} \right) \tag{3.23}$$

If an incompressible materials is considered, i.e. a material having $\upsilon=1/2$, the variable Poisson ratio for the strain rate will become constant according to Eq. (3.21), i.e. $\gamma=1/2$. Therefore for the special case of an incompressible material Eqs. (3.22) and (3.23) become:

$$\dot{\varepsilon}_{11} = \frac{\dot{\sigma}_{11}}{E} + \left| \dot{\varepsilon}_{11} \right| \left| \frac{\sigma_{11} - \beta_{11}}{Y} \right|^{n-1} \left(\frac{\sigma_{11} - \beta_{11}}{Y} \right) \tag{3.24}$$

$$\dot{\beta}_{11} = E\alpha + \left| \dot{\varepsilon}_{11} \right| \left| \frac{\sigma_{11} - \beta_{11}}{Y} \right|^{n-1} \left(\frac{\sigma_{11} - \beta_{11}}{Y} \right)$$

Comparison of Eqs. (3.24) and (3.25) with Eqs. (3.3) and (3.4) reveals that the proposed model of hysteretic material behavior results from the tensor formulation of Eqs. (3.19) and (3.20) for the special case of a uniaxial test applied to an incompressible material. Thus we have shown that the 3D model properly reduces to the 1D material model which was used as the starting point of the extension. Later in this paper, results of numerical calculations will be used to show shear behavior and biaxial behavior of this model. However we will next discuss the rate dependent characteristics of the three dimensional model.

SECTION 4
RATE INDEPENDENCE OF THREE-DIMENSIONAL PLASTICITY MODEL

It has been shown thus far that the one dimensional model of hysteretic behavior for plastically defoming materials is rate independent. Since this one dimensional model was extended to a three dimensional tensorial representation, it is of interest to examine the dependence of the 3D model response to rate effects. Recall that the three dimensional model of metal plasticity was given by Eqs. (3.19) and (3.20). These governing equations are rewritten here in another equivalent form for the sake of convenience:

$$\dot{\Sigma}_{ij} = 2G \left[\dot{e}_{ij} - A_1 \sqrt{K_2}\, J_2^{\frac{n-1}{2}}\, \Sigma_{ij} \right] \tag{4.1}$$

where G is the linear isotropic shear modulus defined by $2G = E/(1+\upsilon)$ and where:

$$A_1 = \left[1 + \frac{E\alpha}{3G} \right] \left[\frac{\sqrt{3}}{Y} \right]^n$$

It is through the examination of Eq. (4.1) that the rate independence of this 3D model will be examined.

A widely used means of measuring the rate dependence (or rate independence) of multi-dimensional material models is the special case of proportional loading. The proportional loading which will be used here is defined as one for which the tensor of effective stresses at any instant of time t is given by:

$$\Sigma_{ij}(t) = (\Sigma_{ij})_o \gamma(t) \tag{4.2}$$

where $(\Sigma_{ij})_o$ is an effective stress tensor of constants and $\gamma(t)$ is a monotonically increasing continuous function of time which equals zero at t=0. During this proportional loading the values of the effective stress tensor will change such that all the components of the effective stress tensor will be the same multiple of corresponding values $(\Sigma_{ij})_o$. It follows from Eq. (4.2) and the definition of J_2 that:

$$\dot{\Sigma}_{ij} = \dot{\gamma}(t)\, (\Sigma_{ij})_o$$

$$(J_2)_o = \frac{1}{2}\, (\Sigma_{ij})_o (\Sigma_{ij})_o$$

Therefore Eq. (4.3) becomes:

$$\dot{e}_{ij} = \dot{\gamma}(t)\, \frac{(\Sigma_{ij})_o}{2G} + \gamma^n A_1 \sqrt{K_2}\, (J_2)_o^{\frac{n-1}{2}}\, (\Sigma_{ij})_o \tag{4.3}$$

In this case it is of interest to determine the response of the strain to this loading. However, due to the presence of the positive quantity $\sqrt{K_2}$ in the second term of Eq. (4.3), it is not possible to make a direct observation regarding the dependence of strain on the rate of loading $\dot{\gamma}(t)(\Sigma_{ij})_o$. To address this problem, we proceed by computing the quantity K_2 using Eq. (4.3). Carrying out the algebra, the following is obtained:

$$K_2 = \dot{\gamma}^2 \frac{(J_2)_o}{4G^2} + \dot{\gamma}\gamma^n \frac{A_1 (J_2)_o^{\frac{n-1}{2}}}{G} \sqrt{K_2} + \dot{\gamma}^{2n} A_1^2 (J_2)_o^n K_2$$

It is readily seen that it is possible to determine the quantity $\sqrt{K_2}$ via the quadratic equation. Because γ is a positive increasing function and $\sqrt{K_2}$ is restricted to positive values, the positive root must be used. Therefore:

$$\sqrt{K_2} = \frac{\dot{\gamma} \frac{\sqrt{(J_2)_o}}{2G}}{1 + \gamma^n A_1 (J_2)_o^{\frac{n}{2}}} \tag{4.4}$$

The next step in evaluating the rate dependent features of Eq. (4.1) requires a better understanding of the physical meaning of $\sqrt{K_2}$. This understanding can be gained by making an analogy to the effective plastic strain rate $\tilde{\dot{\varepsilon}}^p$ and effective plastic strain $\tilde{\varepsilon}^p$ which are often used in the field of plasticity [12]. The following equations are used to define these quantities:

$$\tilde{\dot{\varepsilon}}^p = \frac{2}{3}\sqrt{3K_2^p} \qquad , \qquad K_2^p = \frac{1}{2}\dot{\varepsilon}_{ij}^p \dot{\varepsilon}_{ij}^p$$

$$\tilde{\varepsilon}^p = \int_{t_o}^{t} \tilde{\dot{\varepsilon}}^p (t')dt'$$

where ε_{ij}^p is the symmetric tensor of plastic strains, K_2^p is the second invariant of the plastic strain rate tensor $\dot{\varepsilon}_{ij}^p$, and t_o is the time at which plastic deformation begins. Thus it is seen that for the field of plasticity $\sqrt{K_2^p}$ gives a measure of the effective plastic strain rate.

In an analogous manner, an effective deviatoric total strain $\tilde{e}$, and effective deviatoric strain rate $\tilde{\dot{e}}$, are defined here as:

$$\tilde{e} = \int_{t_o}^{t} \tilde{\dot{e}}(t')dt' \qquad , \qquad \tilde{\dot{e}} = \frac{2}{3}\sqrt{3K_2}$$

Note that $\tilde{e}$ is dependent upon the history of total deformation starting at the onset, i.e, t=0. Recall that K_2 was previously defined as $K_2 = (1/2)\,\dot{e}_{ij}\,\dot{e}_{ij}$. Due to the definition of $\tilde{e}$ it is easily seen through differentiation that:

$$\dot{\tilde{e}} = \tilde{\dot{e}}$$

Thus Eq. (4.4) becomes:

$$\frac{3}{2}\,\dot{\tilde{e}} = \frac{\dot{\gamma}\sqrt{(J_2)_o}}{1+\gamma^n A_1 (J_2)_o^{\frac{n}{2}}}$$

It follows immediately that:

$$\frac{d\tilde{e}}{d\gamma} = a\,\frac{1}{1+b\gamma^n} \tag{4.5}$$

where:

$$a = \frac{2}{\sqrt{3}}\,\frac{\sqrt{(J_2)_o}}{G} \qquad , \qquad b = A_1 (J_2)_o^{\frac{n}{2}}$$

The solution of Eq. (4.5) is determined directly by integration. Thus

$$\tilde{e} = \frac{2}{\sqrt{3}\,A_1^{1/n}\,G} \int_0^{A_1^{1/n}\sqrt{(J_2)_o}\gamma} \frac{d\xi}{1+\xi^n} \tag{4.6}$$

It is clear that the effective deviatoric total strain $\tilde{e}$ given in Eq. (4.6) is independent the rate of loading since $\dot{\gamma}$ is not an argument in the solution Eq. (4.6). Thus by the measure of the effective deviatoric total strain and the case of proportional loading, the three dimensional tensorial model of metal plasticity used here is independent of the rate of loading. For the case of other, more complex, situations of multi-dimensional loading such rate independence cannot be shown analytically. However, a variety of numerical examples discussed in [3] which involved non-proportional biaxial strain paths indicated little or no dependence of the model response to the time rate of change of strain.

SECTION 5
MODEL PREDICTIONS FOR ONE-DIMENSIONAL BEHAVIOR IN SHEAR

In this subsection the 3D model will be analyzed for its behavior under shear loading conditions. The shear strain will be prescribed as sinusoidal in time. The only components in the stress or strain tensors which are non-zero are those components representing pure shear deformation in the xy plane of Cartesian space. Thus:

$$\sigma_{ij} = s_{ij} = \begin{bmatrix} 0 & \sigma_{12} & 0 \\ \sigma_{12} & 0 & 0 \\ 0 & 0 & 0 \end{bmatrix} \qquad \beta_{ij} = b_{ij} = \begin{bmatrix} 0 & \beta_{12} & 0 \\ \beta_{12} & 0 & 0 \\ 0 & 0 & 0 \end{bmatrix}$$

$$\varepsilon_{ij} = e_{ij} = \begin{bmatrix} 0 & \varepsilon_{12} & 0 \\ \varepsilon_{12} & 0 & 0 \\ 0 & 0 & 0 \end{bmatrix}$$

Using Eqs. (3.19) and (3.20), computing the associated invariants, considering the non-zero shear components and simplifying, we arrive at the following pair of differential equations which model the shear stress response to applied shear strains:

$$\dot{\sigma}_{12} = \frac{E}{1+\upsilon}\left[\dot{\varepsilon}_{12} - |\dot{\varepsilon}_{12}|\left|\frac{\sigma_{12}-\beta_{12}}{Y/\sqrt{3}}\right|^{n-1}\left[\frac{\sigma_{12}-\beta_{12}}{Y/\sqrt{3}}\right]\right] \tag{5.1}$$

$$\dot{\beta}_{12} = \frac{2}{3}E\alpha|\dot{\varepsilon}_{12}|\left|\frac{\sigma_{12}-\beta_{12}}{Y/\sqrt{3}}\right|^{n-1}\left[\frac{\sigma_{12}-\beta_{12}}{Y/\sqrt{3}}\right] \tag{5.2}$$

Using the material data given previously in Sec. 2 for A-36 steel, taking sinusoidal control of the strain as $\varepsilon_{12} = A \sin \omega t$ with A = 0.16 in/in and ω = 1 cycle/sec, and using n = 3, the shear response was computed numerically. The results of these computations are plotted in Figure 5-1 and show the shear stress-strain hysteretic response. The numerical data reveal that the yield level in shear is reduced from the yield level in tension (or compression) by a factor of $1/\sqrt{3}$ (i.e. Y_s = 17.3 ksi). The von Mises like yield condition is manifested because of the second invariant formulation of the model. The slope of the elastic regions of the σ_{12}-ε_{12} curve in Figure 5-1 reproduces the expected value of 2G = E/(1+υ) = 21111 ksi. The inelastic modulus is predicted by the response as 368 ksi. This value is reduced from the uniaxial inelastic modulus by a factor of 1.5. Thus it is seen that the shear properties of plastically deforming materials are nicely reproduced when using the 3D model of metal plasticity (Eqs. (3.19) and (3.20).

Thus it can be said for the shear case that initial yielding is predicted in a manner which follows the von Mises criterion and is due to the second invariant formulation inherent to the 3D model. Also, the shear modulus in the elastic regime is predicted according to elasticity theory, i.e. 2G =

$E/(1+\upsilon)$. The inelastic modulus in shear reduces from that of the uniaxial direction by the factor of 1.5 thus indicating that incompressible behavior is being calculated for the inelastic deformation (note that the Poisson ratio was not taken as .5 in deducing the shear equations).

$\varepsilon_{12} = A \sin \omega t$

Y = 30 ksi ν = 0.35 (for uniaxial dir.)

E = 28500 ksi (for uniaxial dir.)

ω =1 A = .016

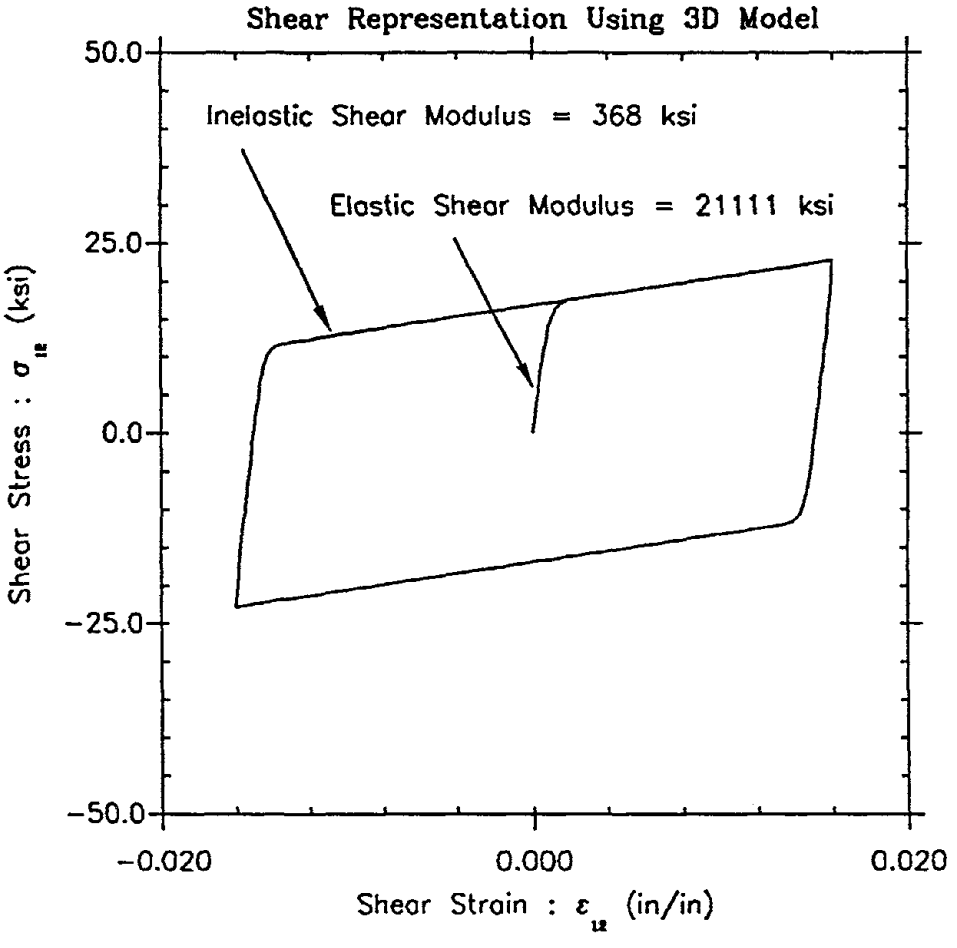

FIGURE 5-1 Predicted Shear Response Based On 3D Plasticity Model.

SECTION 6
BIAXIAL RESPONSE AND COMPARISON TO PUBLISHED RESULTS

Thus far the capabilities of the model of metal plasticity have been demonstrated for the one dimensional cases of uniaxial cyclic loading and cyclic shear loading. It is also of interest to examine the behavior of this model for more general cyclic multi-axial loading conditions involving inelastic deformation. For this purpose, the response of 3D model will be evaluated for biaxial loading conditions.

Published work pertaining to the biaxial loading of metals will be used in this section as a basis for comparison of theoretical predictions to actual experimental results. Multi-axial proportional strain paths are obtained when all components in the strain tensor ε_{ij} change in concert. Thus proportional strain paths are defined by $\varepsilon_{ij} = \varepsilon^{o}_{ij} z(t)$ where ε^{o}_{ij} is a tensor of constant strains and z(t) is a continuous function of time. More complex nonproportional strain paths will be considered in this subsection. In a recent Ph.D. dissertation, Sugiura [17] conducted non-proportional biaxial tests on A-36 structural steel. Also, biaxial test results on copper are presented in [18] (also see [19]). Both studies involve the application of cyclic, non-proportional axial-torsional strain paths. The strain paths from these studies will be used, along with the published experimental responses from [17] and [19] to evaluate the predictive capability of the three-dimensional model of metal plasticity.

The test samples used in [17] and [18] were thin walled hollow cylindrical shafts and were loaded in combined axial tension-compression and torsion. Based on the design of the test samples the state of shear stress resulting from the applied torsion of the shaft is considered uniform in the test region at each instant of time. Therefore the following tensors of stress, backstress, and strain will apply to the biaxial loading configuration described above:

$$\sigma_{ij} = \begin{bmatrix} \sigma_{11} & \sigma_{12} & 0 \\ \sigma_{12} & 0 & 0 \\ 0 & 0 & 0 \end{bmatrix} \qquad \beta_{ij} = \begin{bmatrix} \beta_{11} & \beta_{12} & 0 \\ \beta_{12} & 0 & 0 \\ 0 & 0 & 0 \end{bmatrix}$$

$$\varepsilon_{ij} = \begin{bmatrix} \varepsilon_{11} & \varepsilon_{12} & 0 \\ \varepsilon_{12} & -\delta\varepsilon_{11} & 0 \\ 0 & 0 & -\delta\varepsilon_{11} \end{bmatrix} \qquad \dot{\varepsilon}_{ij} = \begin{bmatrix} \dot{\varepsilon}_{11} & \dot{\varepsilon}_{12} & 0 \\ \dot{\varepsilon}_{12} & -\gamma\dot{\varepsilon}_{11} & 0 \\ 0 & 0 & -\gamma\dot{\varepsilon}_{11} \end{bmatrix}$$

The coefficients δ and γ represent the Poisson effect associated with the lateral deformation and, in general, are variable when inelastic deformations are involved. Computation of the invariants $\sqrt{3K_2}$ and $\left(3J_2^{o}\right)^{(n-1)/2}$ yield:

$$\sqrt{3K_2} = \sqrt{(1+\gamma)^2 \dot{\varepsilon}_{11}^2 + 3\dot{\varepsilon}_{12}^2} \tag{6.1}$$

$$\left(3J_2^0\right)^{\frac{n-1}{2}} = \left[\left(\frac{\sigma_{11} - \beta_{11}}{Y}\right)^2 + 3\left(\frac{\sigma_{12} - \beta_{12}}{Y}\right)^2\right]^{\frac{n-1}{2}} \tag{6.2}$$

Utilizing Eqs. (3.19) and (3.20) for the uniaxial response in the x direction of Cartesian coordinates and also for the shear response in the xy plane, the following equations are arrived at to govern the biaxial loading problem:

$$\dot{\varepsilon}_{11} = \frac{\dot{\sigma}_{11}}{E} + \frac{2}{3} D_p \left(\frac{\sigma_{11} - \beta_{11}}{Y}\right) \tag{6.3}$$

$$\dot{\varepsilon}_{11} = \frac{1+\upsilon}{E} \dot{\sigma}_{12} + D_p \left(\frac{\sigma_{12} - \beta_{12}}{Y}\right) \tag{6.4}$$

$$\dot{\beta}_{11} = \frac{2}{3} E\alpha D_p \left(\frac{\sigma_{11} - \beta_{11}}{Y}\right) \tag{6.5}$$

$$\dot{\beta}_{12} = \frac{2}{3} E\alpha D_p \left(\frac{\sigma_{12} - \beta_{12}}{Y}\right) \tag{6.6}$$

where D_p defines the following product of invariant functions:

$$D_p = \sqrt{3K_2}\left(3J_2^0\right)^{\frac{n-1}{2}} \tag{6.7}$$

In Eqs. (6.3) and (6.4) the growth of D_p results in an increased contribution to the evolution of the inelastic portions of ε_{11} and ε_{12}. Since plastic deformation is governed by the dislocation glide mechanism we know that no change in volume (zero dilatation) is associated with this mechanism. Thus plastic flow can be taken as incompressible. This is achieved by setting $\gamma = .5$ in Eq. (6.1). Doing this, Eq. (6.1) becomes:

$$\sqrt{3K_2} = \sqrt{\frac{9}{4}\dot{\varepsilon}_{11}^2 + 3\dot{\varepsilon}_{12}^2}$$

The problem to be solved is one wherein a strain path in biaxial strain space is prescribed and the resulting stress response is desired. Therefore Eqs. (6.3) to (6.6) are rearranged as follows:

$$\dot{\sigma}_{11} = E\left[\dot{\varepsilon}_{11} - \frac{2}{3} D_p \left(\frac{\sigma_{11} - \beta_{11}}{Y}\right)\right] \tag{6.8}$$

$$\dot{\sigma}_{12} = 2G\left[\dot{\varepsilon}_{12} - D_p\left(\frac{\sigma_{12} - \beta_{12}}{Y}\right)\right] \tag{6.9}$$

$$\dot{\beta}_{11} = \frac{2}{3} E\alpha\, D_p\left(\frac{\sigma_{11} - \beta_{11}}{Y}\right) \tag{6.10}$$

$$\dot{\beta}_{12} = \frac{2}{3} E\alpha\, D_p\left(\frac{\sigma_{12} - \beta_{12}}{Y}\right) \tag{6.11}$$

where Eq. (6.7) now becomes:

$$D_p = \sqrt{\frac{9}{4}\dot{\varepsilon}_{11}^2 + 3\dot{\varepsilon}_{12}^2}\left[\left(\frac{\sigma_{11} - \beta_{11}}{Y}\right)^2 + 3\left(\frac{\sigma_{12} - \beta_{12}}{Y}\right)^2\right]^{\frac{n-1}{2}} \tag{6.12}$$

Solution of the biaxial problem subsequently involves the numerical integration of Eqs. (6.8) through (6.11) for a given strain path in biaxial space.

We first consider a non-proportional strain path as presented in [17]. This path is shown in Figure 6-1. Figure 6-2 shows the concurrent time history of the applied axial and shear strains for this biaxial path. The experimental response of A-36 structural steel to this biaxial strain path is shown in Figure 6-3 and 6-4 for the axial and shear directions respectively. The solid lines on Figure 6-3 and 6-4 are theoretical predictions from [17] for the biaxial response and are based upon the use of an endochronic theory of plasticity. These theoretical responses are specific to the discussion in [17] and are not to be confused with the theoretical predictions being presented here. Thus we are only interested in the experimental responses given by the dashed lines in Figures 6-3 and 6-4. Numerical integration of Eqs. (6.8)-(6.11) for the strain input of Figures 6-1 and 6-2 was carried out and the resulting predictions of the axial and shear stress responses are shown in Figures 6-5 and 6-6. The material data which was used in Eqs. (6.8) thru (6.11) was given previously for A-36 steel.

Comparison of the predictions given in Figures 6-5 and 6-6 to the experimental response given in Figures 6-3 and 6-4 allows for a number of observational remarks to be made. It is immediately recognized that the biaxial model of plasticity gives a very good overall reproduction of the general shape of the experimental response. Transition from the elastic to plastic regime is somewhat sharper for the model. Notice that the axial experimental response of Figure 6-3 does not show the initial ascending branch from the zero stress state. This is because the test sample was initially cycled through a repeated pattern of axial strain which produced a kinematic stabilization of the hysteresis loop. The stabilization was carried out prior to biaxial loading and was applied only in the axial direction [17]. Referring back to Figures 6-3 to 6-6, careful comparisons reveal that the model under-predicts experimental stress response levels by approximately 20%. This deficiency can be improved, however, by modifying the value of Y

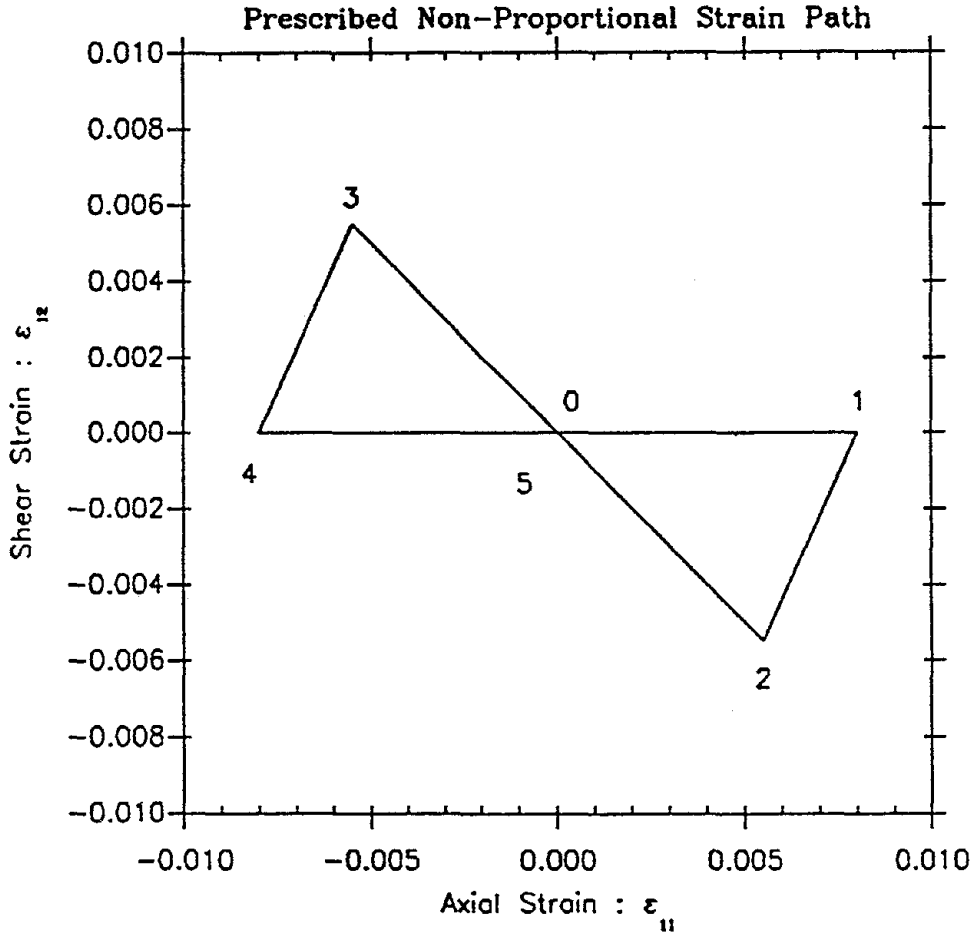

FIGURE 6-1 Cyclic Non-Proportional Strain Path as Used in [17].

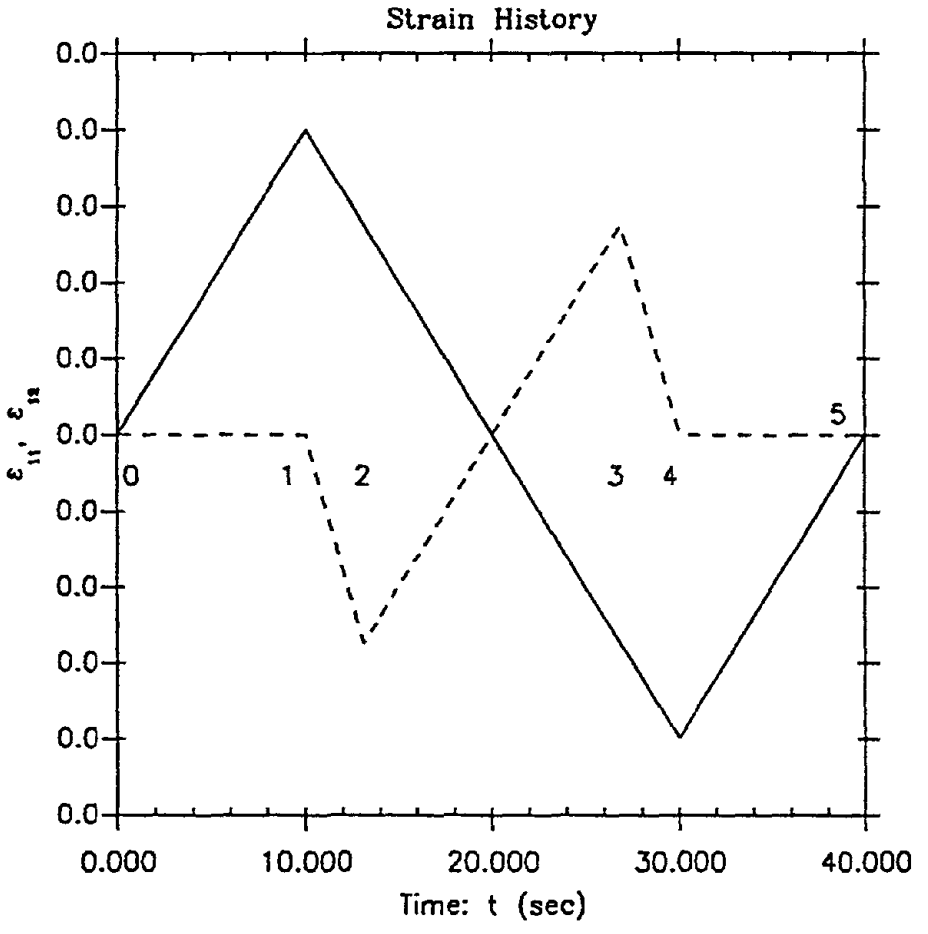

FIGURE 6-2 Time History of Axial Strain (solid line) and Shear Strain (dashed line). Data are as Presented in [17].

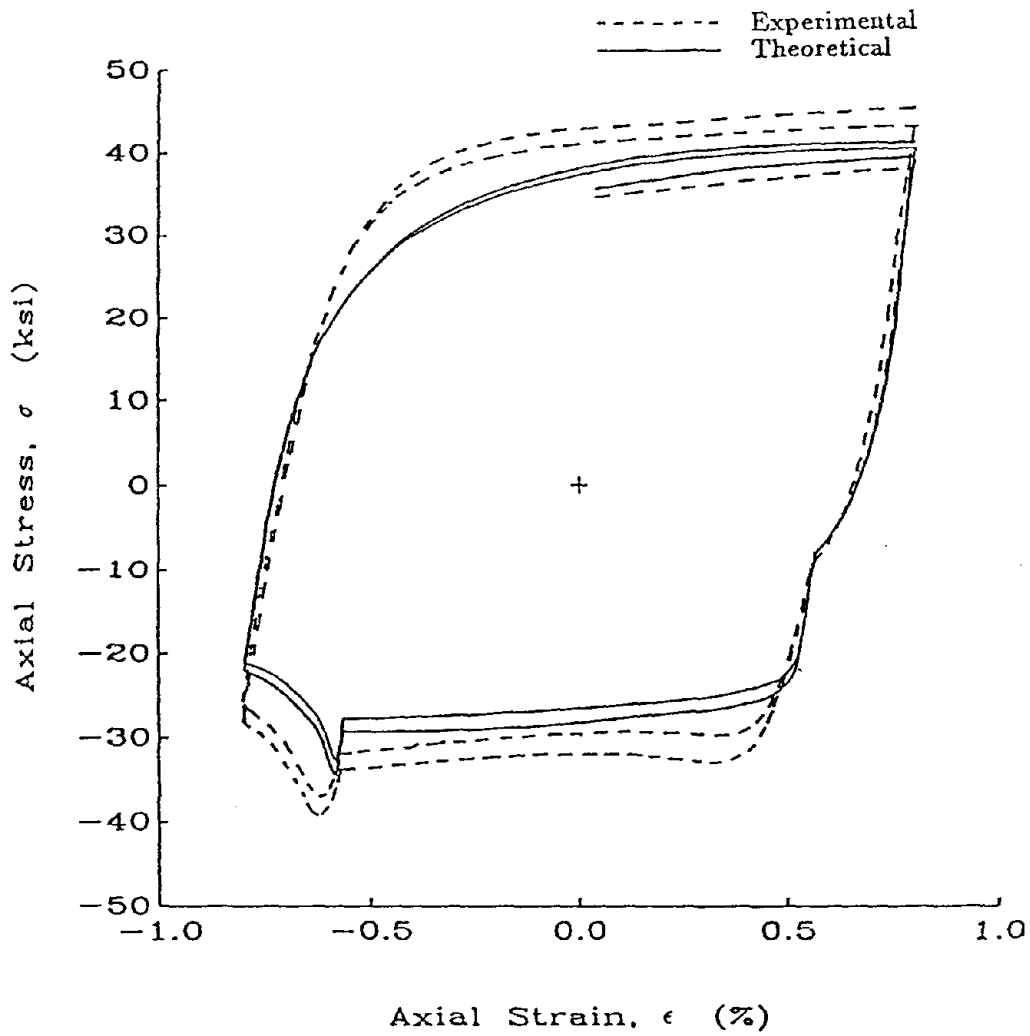

FIGURE 6-3 Axial Response of A-36 Steel to Biaxial Loading. Data are as Presented in [17].

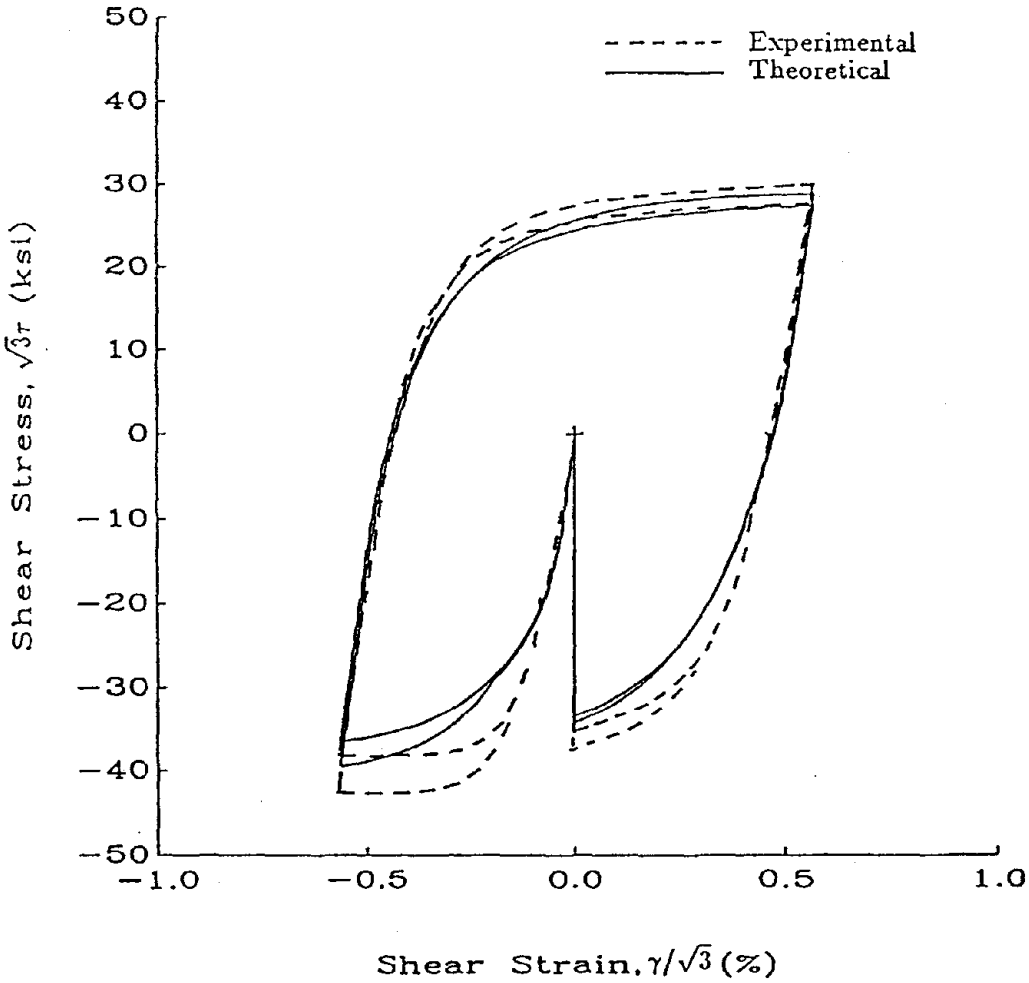

FIGURE 6-4 Shear Response of A-36 Steel to Biaxial Loading. Data are as Presented in [17].

Y = 30 ksi ν = 0.35

E = 28500 ksi

α = 0.0197 n = 7

Non-proportional Strain Path is prescribed

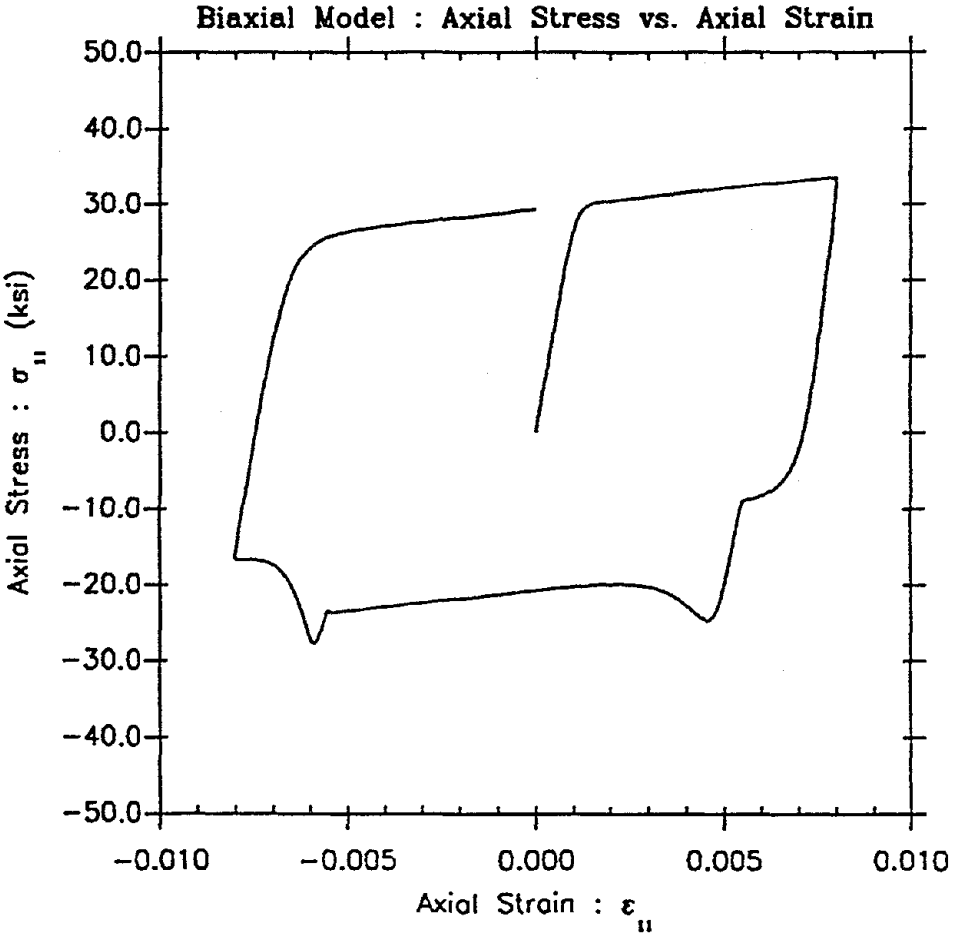

Figure 6-5 Prediction of Axial Response for A-36 Steel.

Y = 30 ksi ν = 0.35

E = 28500 ksi

α = 0.0197 n = 7

Non-proportional Strain Path is prescribed

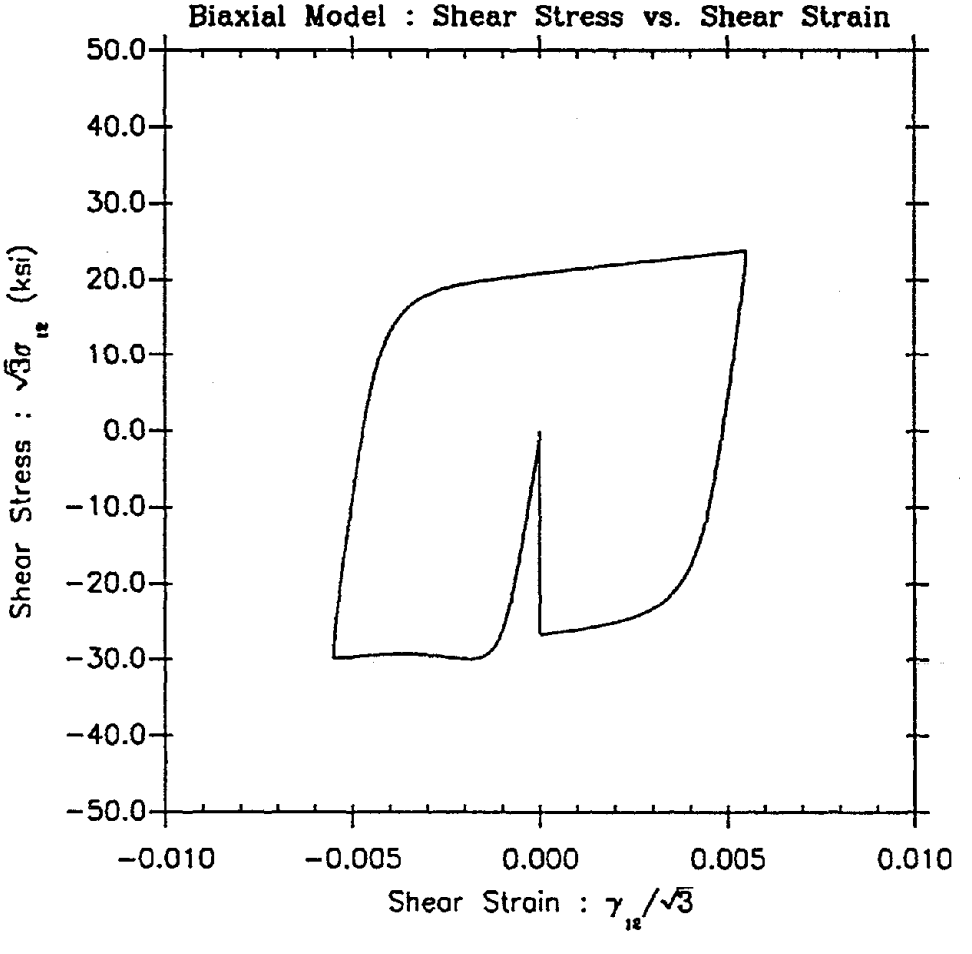

Figure 6-6 Prediction of Shear Response for A-36 Steel.

used in Eqs. (6.8) through (6.11). In the calculations made up to this point, a yield stress of Y = 30 ksi was used to represent initial axial yielding and was taken from [15]. However, if one returns to [17] and examines the initial axial hysteretic response of the sample before biaxial loading, it is seen that the shape of the hysteresis loop stabilizes to a configuration wherein the yield point is raised above its initial value of 30 ksi. This increased axial yield point corresponds to a .2% offset in strain and has a value of 34 ksi. Using this increased value of Y in calculations causes the stresses in the model response to increase significantly such that the new stress levels under-predict actual stress levels by approximately 9%. As such, a significant improvement in modeling capability is achieved through the use of the yield point corresponding to a .2% offset in strain for cyclically stabilized hysteresis patterns. In the next set of calculations to be considered, the axial yield point will be taken from a stabilized axial hysteresis loop pattern in order to demonstrate this effect. Also, the use of another biaxial strain path will give an additional means of model verification.

The next example which will be considered involves comparison of the plasticity model to experimental biaxial results for copper. These results were originally published by Lamba and Sidebottom [18] and were used by Freed in his more recent study [19]. These studies present the experimental stress response of copper to a specified non-proportional biaxial strain path. The material data which was used here in model calculations was obtained from a cyclically stabilized hysteretic response for copper as given in [19]. From these results the yield stress at a .2% offset in strain was measured as Y = 200 MPa and the slope of the inelastic region of deformation was measured approximately as E_y = 500 MPa. The elastic modulus and Poisson ratio for copper are E = 126000 MPa and υ = .34 respectively. This material data is now summarized as follows:

Material Data for Copper [22]

Material Property	**Symbol**	**Value**
Young's Modulus	E	126000 MPa
Yield Stress	Y	200 MPa
Plastic Modulus	E_y	500 MPa
Poisson Ratio	υ	.34

Using the above data the constant α is computed as α = .004.

The non-proportional biaxial strain path originally used in [18] is shown in Figure 6-7. Also shown in this figure is the experimental stress response of copper to this nonproportional cyclic straining. The strain path of Figure 6-7 was used as input to a FORTRAN algorithm which integrated Eqs. (6.8)-(6.11) numerically. As with previously shown calculations, conventional fourth order Runge-Kutta numerical integration was employed. Each segment of the strain path (0-1,1-2,...7-8) was traced in 60 time steps thus corresponding to the rate of loading used in the original experiment. Based on the results of these calculations, the theoretical prediction for the stress response of copper is shown in Figure 6-8. Comparison of Figures 6-8 and 6-9 shows

that an excellent correlation is obtained between the theoretical prediction and the experimental response. It is clearly evident that the predicted response has the same shape as the experimental response. Also, careful comparisons show that for corresponding points on the plots of Figures 6-7 and 6-8, both axial and shear stresses are predicted to within 10% of experimental values.

Note from Figure 6-7 that each segment of the biaxial strain path (0-1,1-2,...) was applied in 60 seconds during the original experiments. The same rate of strain application was used in the computations for the model response shown in Figure 6-8. To measure the rate sensitivity of the biaxial model, the shape of the biaxial strain path was maintained while the rate of strain application was increased by a factor of 100 to .6 seconds for each path segment. The resulting response in stress space of the material model to the increase rate of strain application was unaltered from that given previously in Figure 6-8. Thus, through these numerical calculations, the model of plasticity is again shown to be insensitive to changes in strain rate.

In the comparisons undertaken here, the model of plasticity was compared only to cyclically stable material responses. The predictive capability of this model is indeed well suited for such comparative purposes. Another beneficial aspect of the plasticity model is its simple form. Mathematically, it is much less complicated than most other viscoplastic and unified theories because it contains only one evolving internal variable, i.e. the backstress. The model is therefore useful in the physical modeling of rate independent materials and devices as used in earthquake engineering and structural damping.

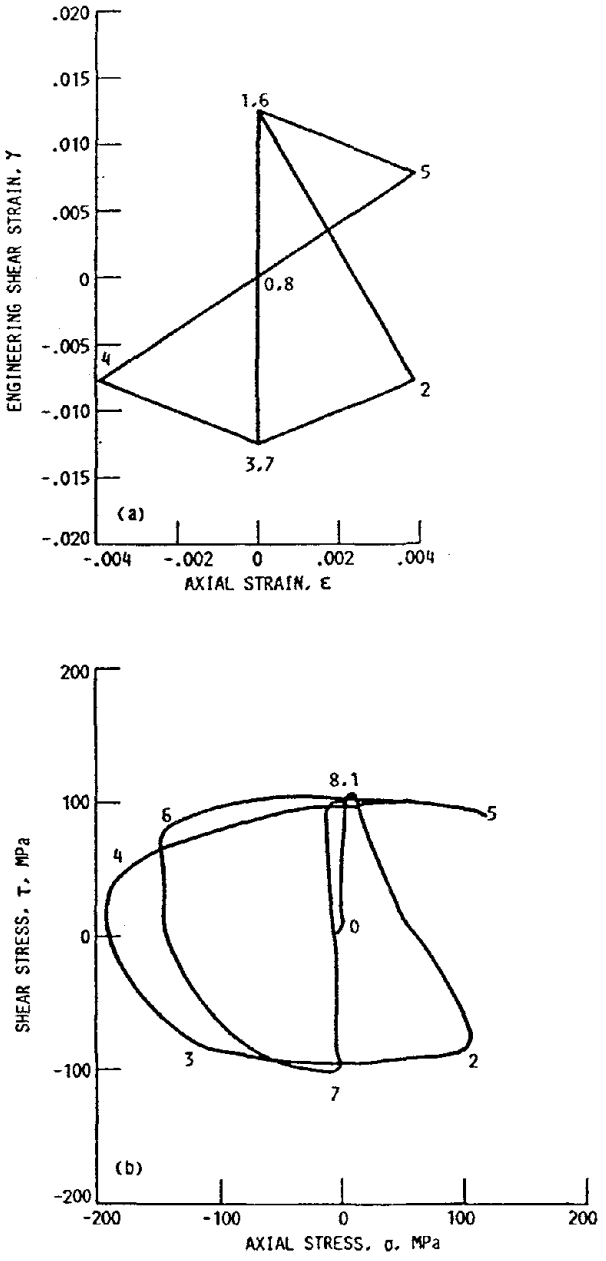

(a) Strain control program.
(b) Experimental stress response.

Cyclic, nonproportional, axial-torsional test of copper at room temperature. Test specimen cycled to isotropic saturation prior to testing. Path segments sequenced from 0 — 1 — 2 — ... — 8. Each path segment applied in 60 s.

Figure 6-7 Biaxial Strain Path and Experimental Stress Response of Copper. Data are Presented as in [19].

$Y = 200$ MPa $\quad \nu = 0.34$

$E = 126000$ MPa

$\alpha = 0.004 \quad n = 5$

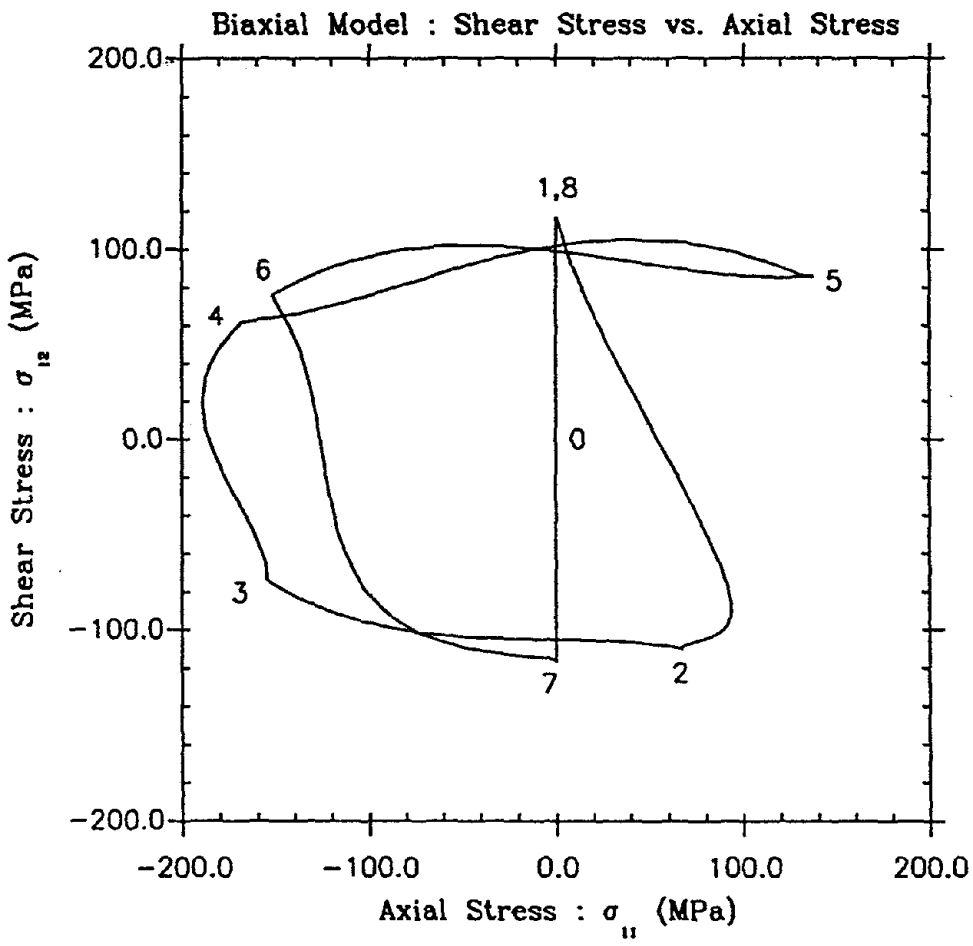

Figure 6-8 Predicted Biaxial Stress Response for Copper.

SECTION 7
SUMMARY

In this paper Ozdemir's one dimensional model of rate-independent hysteretic behavior was extrapolated to a three-dimensional set of tensorial equations. These equations form a rate independent law of plasticity which is of the evolutionary type and is based on the concept of overstress.

Because the model contains only one evolutionary internal variable, it is relatively simple with respect to many other models of inelastic material behavior. Also, the model contains physically motivated constants in its formulation. Thus it is potentially very useful for multi-axial material response analyses.

In order to verify the theory computational results were presented for cyclic one-dimensional uniaxial and shear responses, as well as for two dimensional cyclic biaxial responses. It was shown that the uniaxial models properly reproduce the initial axial yield point, the axial elastic and inelastic moduli, and the Bauschinger effect. This was demonstrated both in analytical and computational cases. The shear response of the plasticity model was shown to display yielding behavior which follows the criterion of Von Mises. This is due to the second invariant type formulation which is contained in the 3D plasticity law. Biaxial responses for the plasticity model compared very well with experimental responses from the open literature. Also, the three-dimensional model of plasticity was shown to possess rate independent characteristics in both numerical and analytical cases. Finally, in the appendix the 3D model of plasticity was shown to be consistent within the framework of thermodynamics.

SECTION 8
REFERENCES

1. Kelly, J.M., 1986, "Aseismic Base Isolation: Review & Bibliography," Soil Dynamics and Earthquake Engineering Vol. 5(3), pp. 202-216.

2. Lin, R.C., Liang, Z., Soong, T.T., and Zhang, R.H., 1988, "An Experimental Study of Seismic Structural Response with Added Viscoelastic Dampers," National Center for Earthquake Engineering Research, Technical Report NCEER-88-0018, Buffalo, NY.

3. Graesser, E.J., 1990, "Multi-Dimensional Modeling of Hysteretic Materials Including Shape Memory Alloys: Theory and Experiment," Ph.D. Dissertation, SUNY at Buffalo, Buffalo, New York.

4. Ozdemir, H., 1976, "Nonlinear Transient Dynamic Analysis of Yielding Structures," Ph.D. Dissertation, U.C. Berkeley, Berkeley, California.

5. Wen, Y.K., 1976, "Method for Random Vibration of Hysteretic Systems," Journal of the Engineering Mechanics Division, ASCE, Vol. 102 (EM2), pp. 249-263.

6. Bhatti, M.A., Pister, K.S. and Polak, E., 1978, "Optimal Design of an Earthquake Isolation System," Earthquake Engineering Research Center, Report No. UCB/EERC-78/22, Berkeley, California.

7. Krempl, E., 1987, "Models of Viscoplasticity - Some Comments on Equilibrium (Back) Stress and Drag Stress," Acta Mechanica, Vol. 69, pp. 25-42.

8. Miller, A.K. (ed.), 1987, Unified Constitutive Equations for Creep and Plasticity, Elsevier Applied Science.

9. Constantinou, M.C. and Tadjbakhsh, I.G., 1985, "Hysteretic Dampers in Base Isolation: Random Approach," Journal of Structural Engineering, ASCE, Vol. iii, No. 4, pp. 705-721.

10. Baber, T.T., and Noori, M.N., 1985, "Random Vibration of Degrading, Pinching Systems," Journal of Engineering Mechanics", ASCE, Vol. iii, No. 8, pp. 1010-1026.

11. Prager, W., 1945, "Strain Hardening Under Combined Stresses," J. Appl. Physics, Vol. 16, pp. 837.

12. Shames, I.H. and Cozzarelli, F.A., 1991, Elastic and Inelastic Stress Analysis, Prentice-Hall Inc.

13. Constantinou, M.C. and Adnane, M.A., 1987, "Dynamics of Soil-Base-Isolated Structure Systems: Evaluation of Two Models for Yielding Systems," Report to National Science Foundation, Dept. of Civ. Engrg., Drexel Univ., Philadelphia, PA.

14. Constantinou, M., A. and Reinhorn, A., 1990, "Teflon Bearings in Base Isolation. II: Modeling," Journal of Structural Engineering, Vol. 116 (2), pp. 455-474.

15. Chang, K.C. and Lee, G.C., 1986, "Biaxial Properties of Structural Steel Under Non-proportional Loading," Journal of Engineering Mechanics, ASCE, Vol. 112 (8).

16. Chang, W.P. and Cozzarelli, F.A., 1977, "On the Thermodynamics of Nonlinear Single Integral Representations of Thermoviscoelastic Materials with Applications to One-Dimensional Wave Propagation," Acta Mechanica, Vol. 25, pp. 187-206.

17. Sugiura, K., 1988, "Low Cycle Fatigue of Structural Steel," Ph.D. Dissertation, S.U.N.Y. at Buffalo.

18. Lamba, H.S. and Sidebottom, O.M., 1978, "Cyclic Plasticity for Nonproportional Paths: Part 2-Comparison With Predictions of Three Incremental Plasticity Models," J. Eng. Mat. Tech., Trans ASME, Vol. 100, No. 1, pp. 104-111.

19. Freed, A.K., 1988, "Thermoviscoplastic Model With Application to Copper," NASA Technical Paper 2845, 1988.

20. Boley, B.A. and Weiner, J.H., 1953, Theory of Thermal Stresses, Wiley.

21. Malvern, L.E., 1969, Introduction to the Mechanics of a Continuous Medium, Prentice-Hall.

22. Coleman, B.D., 1964, "Thermodynamics of Materials with Memory," Arch. Rat. Mech., Vol. 17, pp. 1-46.

23. Burke, K. and Cozzarelli, F.A., 1984, "On the Thermodynamic Foundations of Strain Dependent Creep Damage and Rupture in Three Dimensions," Int. J. Solids Structures, Vol. 20, No. 5, pp. 487-497.

24. Rice, J., 1970, "On the Structure of Stress-Strain Relations for Time Dependent Plastic Deformation in Metals," J. Appl. Mech., Trans. ASME, Vol. 37, No. 3, pp. 728-737.

25. Ponter, A.R.S. and Leckie, F.A., 1976, "Constitutive Relationships for the Time-Dependent Deformation of Metals," J. Eng. Mat. Tech., Trans. ASME, Vol. 98, No. 1, pp. 47-51.

26. Robinson, D.N., 1984, "Constitutive Relationships for Anisotropic High Temperature Alloys," Nuclear Engineering and Design, Vol. 83, pp. 389-396.

27. Onat, E.T. and Fardshisheh, F., 1972, "Representation of Creep in Metals," Tech. Report ORNL-4783, U.S. Atomic Energy Commission, Oak Ridge Nat'l. Lab.

28. Onat, E.T. and Fardshisheh, F., 1973, "Representation of Creep, Rate Sensitivity and Plasticity," SIAM J. Appl. Math., Vol. 25, No. 3, pp. 522-538.

29. Freed, A.D. and Chaboche, J.L., "Viscoplasticity: A Thermodynamic Formulation," to appear J. Appl. Mech.

APPENDIX A
THERMODYNAMIC CONSIDERATIONS

In this appendix the three dimensional model of plasticity will be studied from the perspective of thermodynamics. Specifically, the equations which were set forth earlier will be compared to a general functional form for flow and evolutionary equations which are based upon the laws of thermodynamics.

In a review of the literature the aspect of thermodynamically based constitutive relationships for solid materials was of interest. Many technical books and articles have been published which fall under this general category. For example, classical textbooks such as those by Boley and Weiner [20] and Malvern [21] state the underlying principles which lead to the laws of thermodynamics for a continuum. Many constitutive relationships in the areas of viscoelasticity and continuum damage mechanics are either based upon thermodynamic foundations or are proven to be thermodynamically consistent. Example of such work include [16,22,23].

In the study of plasticity and viscoplasticity many theoretical developments are based upon the assumption of a potential function existing in stress space from which flow and evolutionary equations are derivable. Examples of such developments are given in [24,25,26]. The development of viscoplastic theories from thermodynamic considerations is less widespread. Onat and Fardshisheh [27,28] have done work pertaining to thermodynamics and plasticity. More recently Freed and Chaboche [29] have collaborated to write a paper regarding a thermodynamic formulation specific to viscoplasticity. The concept of internal state variables is used in the thermodynamic foundation as applied to initially isotropic materials.

In the discussion presented herein the goal is to use the laws of thermodynamics to set forth the general function form of the flow and evolutionary equations, and to gain some useful conditions on the equations. the material under consideration is one which is initially in an isotropic, undeformed, and stress free condition. In Cartesian coordinates the strain tensor ε_{ij} is taken to be composed of reversible elastic strains ε_{ij}^{el} and irreversible inelastic strains ε_{ij}^{in} such that the two components added together make up the sum total strain:

$$\varepsilon_{ij} = \varepsilon_{ij}^{el} + \varepsilon_{ij}^{in} \tag{A.1}$$

The thermodynamic state of the material element characterizes its internal structure at any given instant of time. Guided by the development given in [29] and noting the forms of the inelastic strain rate and internal backstress which were developed earlier (see Eqs. (3.19) and (3.20), the thermodynamic state is taken as $\{\varepsilon_{ij}^{el}\ \alpha_\beta,\ \dot{\varepsilon}_{ij},\ T,\ \nabla_i T\}$. Here ε_{ij}^{el} is a measure of the elastic changes in the internal structure of the material, α_β ($\beta = 1,2,...,n$) are a general number of measures for inelastic changes in the internal structure, $\dot{\varepsilon}_{ij}$ is a measure of the time rate of change of total strain (elastic plus inelastic) in the material, T is a measure of the heat in the material, and $\nabla_i T$ is a measure of the heat flow out of the material element.

The first and second laws of thermodynamics brought together in the Clausius-Duhem inequality [21] is now utilized in the thermodynamic development:

$$\dot{S} \geq \frac{1}{T}\left(\dot{U} - \sigma_{ij}\dot{\varepsilon}_{ij} + \frac{q_i}{T}\nabla_i T\right)$$

Here S is the entropy, q_i is the heat flux vector, and U is the internal energy. Next, the decomposition of strain, Eq. (A.1), and the Helmholtz free energy $\Psi = U - ST$ are introduced into the Clausius-Duhem inequality whereby the following result is obtained:

$$\sigma_{ij}\dot{\varepsilon}_{ij}^{in} \geq \dot{\Psi} + S\dot{T} - \sigma_{ij}\dot{\varepsilon}_{ij}^{el} + \frac{q_i}{T}\nabla_i T \tag{A.2}$$

Since the set of variables $\{\varepsilon_{ij}^{el}\ \alpha_\beta,\ \dot{\varepsilon}_{ij},\ T,\ \nabla_i T\}$ is taken as the thermodynamic state and since the internal energy and entropy are dependent upon this state, the Helmholtz potential Ψ must also be a function of these variables, i.e.

$$\Psi = \Psi\left(\varepsilon_{ij}^{el}, \alpha_\beta, \dot{\varepsilon}_{ij}, T, \nabla_i T\right)$$

Thus inequality (A.2) becomes:

$$\sigma_{ij}\dot{\varepsilon}_{ij}^{in} \geq \left[\frac{\partial\Psi}{\partial\varepsilon_{ij}^{el}} - \sigma_{ij}\right]\dot{\varepsilon}_{ij}^{el} + \left[S + \frac{\partial\Psi}{\partial T}\right]\dot{T} + \frac{\partial\Psi}{\partial\varepsilon_{ij}}\ddot{\varepsilon}_{ij} + \sum_{\beta=1}^{n}\frac{\partial\Psi}{\partial\alpha_\beta}\dot{\alpha}_\beta + \frac{\partial\Psi}{\partial(\nabla_i T)}\frac{\partial(\nabla_i T)}{\partial t} + \frac{q_i}{T}\nabla_i T \tag{A.3}$$

In the inequality (A.3) above, the coefficients of the observable variables $\dot{\varepsilon}_{ij}^{el}$, $\dot{T}$, and $\partial(\nabla_i T)\partial t$ are set equal to zero since the inequality must remain valid for arbitrary changes in these variables. This results in the following constitutive equations:

$$\sigma_{ij} = \frac{\partial\Psi}{\partial\varepsilon_{ij}^{el}} \qquad A_\beta = \frac{\partial\Psi}{\partial\alpha_\beta} \qquad g_{ij} = \frac{\partial\Psi}{\partial\ddot{\varepsilon}_{ij}}$$

$$S = -\frac{\partial\Psi}{\partial T} \qquad \frac{\partial\Psi}{\partial(\nabla_i T)} = 0 \tag{A.4}$$

dissipation inequality:

$$\sigma_{ij}\dot{\varepsilon}_{ij}^{in} - \sum_{\beta=1}^{n} A_\beta\dot{\alpha}_\beta - g_{ij}\ddot{\varepsilon}_{ij} - \frac{q_i}{T}\nabla_i T \geq 0 \tag{A.5}$$

and evolution equations:

$$\dot{\varepsilon}_{ij}^{in} = \dot{\varepsilon}_{ij}^{in}\left(\varepsilon_{kl}^{el}, \alpha_\gamma, \dot{\varepsilon}_{kl}, T, \nabla_k T\right)$$

$$\dot{\alpha}_\beta = \dot{\alpha}_\beta\left(\varepsilon_{kl}^{el}, \alpha_\gamma, \dot{\varepsilon}_{kl}, T, \nabla_k T\right)$$

$$\ddot{\varepsilon}_{ij} = \ddot{\varepsilon}_{ij}\left(\varepsilon_{kl}^{el}, \alpha_\gamma, \dot{\varepsilon}_{kl}, T, \nabla_k T\right) \qquad \text{(A.6)}$$

$$q_i = q_i\left(\varepsilon_{kl}^{el}, \alpha_\gamma, \dot{\varepsilon}_{kl}, T, \nabla_k T\right)$$

Taking q_i as independent of ε_{ij}^{el} α_β, and T, and also taking $\dot{\varepsilon}_{ij}^{in}$ and $\dot{\alpha}_\beta$ as independent of $\nabla_i T$, the dissipation inequality (A.5) is separated into intrinsic and thermal dissipation inequalities given respectfully as:

$$\sigma_{ij}\,\dot{\varepsilon}_{ij}^{in} - \sum_{\beta=1}^{n} A_\beta\,\dot{\alpha}_\beta - g_{ij}\,\ddot{\varepsilon}_{ij} \geq 0$$

and

$$\frac{q_i}{T}\,\nabla_i T \leq 0$$

The heat flux is taken to obey the Fourier heat conduction law:

$$q_i = -\,k_{ij}\,\nabla_j T$$

where k_{ij} is the positive definite conductivity tensor.

For the formulation of plastic deformation being studied in this paper, there is no consideration of thermal stress effects. Also, heat flow problems are not being studied within the contect of this work. Thus the constitutive Eqs. (A.4) simplify to:

$$\sigma_{ij} = \frac{\partial \Psi}{\partial \varepsilon_{ij}^{el}} \qquad A_\beta = \frac{\partial \Psi}{\partial \alpha_\beta} \qquad g_{ij} = \frac{\partial \Psi}{\partial \dot{\varepsilon}_{ij}} \qquad \text{(A.7)}$$

with the intrinsic dissipation inequality:

$$\sigma_{ij}\,\dot{\varepsilon}_{ij}^{in} - \sum_{\beta=1}^{n} A_\beta\,\dot{\alpha}_\beta - g_{ij}\,\ddot{\varepsilon}_{ij} \geq 0 \qquad \text{(A.8)}$$

The evolutionary Eqs. (A.6) become:

$$\dot{\varepsilon}_{ij}^{in} = \dot{\varepsilon}_{ij}^{in}\left(\varepsilon_{kl}^{el},\, \alpha_\gamma,\, \dot{\varepsilon}_{kl}\right)$$

$$\dot{\alpha}_\beta = \dot{\alpha}_\beta\left(\varepsilon_{kl}^{el},\, \alpha_\gamma,\, \dot{\varepsilon}_{kl}\right)$$

$$\ddot{\varepsilon}_{ij} = \ddot{\varepsilon}_{ij}\left(\varepsilon_{kl}^{el},\, \alpha_\gamma,\, \dot{\varepsilon}_{kl}\right) \qquad \text{(A.9)}$$

Following the development in [29], the Helmholtz free energy is taken as the sum of separate potentials corresponding to elastic and inelastic deformation:

$$\Psi = \Psi\left(\varepsilon_{ij}^{el},\, \alpha_\beta,\, \dot{\varepsilon}_{ij}\right) = \Psi^{el}\left(\varepsilon_{ij}^{el}\right) + \Psi^{in}\left(\alpha_\beta, \dot{\varepsilon}_{ij}\right)$$

By taking Ψ^{el} to follow from elasticity theory:

$$\Psi^{el} = \frac{1}{2}\, \varepsilon_{ij}^{el}\, D_{ijkl}\, \varepsilon_{kl}^{el}$$

It follows that the first constitutive equation of the set (A.7) is:

$$\sigma_{ij} = D_{ijkl}\, \varepsilon_{kl}^{el} \qquad \text{or} \qquad \varepsilon_{ij}^{el} = D_{ijkl}^{-1}\, \sigma_{kl}$$

where D_{ijkl} is the general symmetric tensor of elastic moduli. The second potential Ψ^{in} is postulated as:

$$\Psi^{in} = \frac{1}{2} \sum_{\beta=1}^{n} \sum_{\gamma=1}^{n} \alpha_\beta\, H_{\beta\gamma}\, \alpha_\gamma + \frac{1}{2}\, \dot{\varepsilon}_{ij}\, P_{ijkl}\, \varepsilon_{kl}$$

The first term in this expression is taken following [29] where $H_{\beta\gamma}$ is the symmetric matrix of hardening coefficients. The second term is postulated here in an analogous way with P_{ijkl} as a general symmetric tensor of additional hardening constants. Thus from the remaining constitutive Eqs. (A.7):

$$A_\beta = \sum_{\gamma=1}^{n} H_{\beta\gamma}\, \alpha_\beta \qquad \text{or} \qquad \alpha_\beta = \sum_{\gamma=1}^{n} H_{\beta\gamma}^{-1}\, A_\beta$$

$$g_{ij} = P_{ijkl}\, \dot{\varepsilon}_{kl}$$

The goal here is to show that the formulation set forth in the body of this paper is thermodynamically admissible for the thermodynamic state being considered. Using the above results, the evolutionary Eqs. (A.9) can be reexpressed as follows:

$$\dot{\varepsilon}_{ij}^{in} = \dot{\varepsilon}_{ij}^{in}\left(\sigma_{kl}, A_\gamma, \dot{\varepsilon}_{kl}\right)$$

$$\dot{\alpha}_\beta = \dot{\alpha}_\beta\left(\sigma_{kl}, A_\gamma, \dot{\varepsilon}_{kl}\right)$$

$$\ddot{\varepsilon}_{ij} = \ddot{\varepsilon}_{ij}\left(\sigma_{kl}, A_\gamma, \dot{\varepsilon}_{kl}\right) \qquad \text{(A.10)}$$

Here the tensor of elastic strains are replaced by the stress tensor σ_{ij} and the conjugate thermodynamic forces A_γ are used in place of the internal displacements α_γ. These substitutions do not result in any loss of generality. Thus we have now arrived at the fundamental set of equations to which the three dimensional model of plasticity will be compared.

Referring back to Eqs. (3.19) and (3.20) the following evolutionary equations for inelastic strain and internal backstress are as follows:

$$\dot{\varepsilon}_{ij}^{in} = \sqrt{3K_2}\,(3J_2^0)^{\frac{n-1}{2}}\left[\frac{s_{ij} - b_{ij}}{Y}\right] \qquad \text{(A.11)}$$

$$\dot{b}_{ij} = \frac{2}{3}E\alpha\sqrt{3K_2}\,(3J_2^0)^{\frac{n-1}{2}}\left[\frac{s_{ij} - b_{ij}}{Y}\right] \qquad \text{(A.12)}$$

where s_{ij} and b_{ij} were defined earlier as the stress and backstress deviator tensors, J_2^0 was defined as the second invariant of the overstress deviator tensor, i.e., $J_2^0 = (1/2Y^2)(s_{ij}-b_{ij})(s_{ij}-b_{ij})$ and the second invariant of the total strain rate deviator tensor was given as $K_2 = (1/2)\dot{e}_{ij}\dot{e}_{ij}$. Eq. (A.12) describes the evolution of the backstress deviator. The material constant α in Eq. (A.12) is not to be confused with the internal variables α_β. Now, the conjugate displacement to the backstress deviator is defined simply as $f_{ij} = b_{ij}/E\alpha$. Thus the evolutionary equation for the internal strains which results from the growth of backstress is:

$$\dot{f}_{ij} = \frac{2}{3}\sqrt{3K_2}\,(3J_2^0)^{\frac{n-1}{2}}\left[\frac{s_{ij} - b_{ij}}{Y}\right]$$

Note from the formulation given here (for initially isotropic materials) that:

$$D_{ijkl}^{-1} = \frac{1+\upsilon}{E}\,\delta_{ij}\delta_{jl} - \frac{\upsilon}{E}\delta_{ij}\delta_{kl}$$

$$A_\beta \longrightarrow b_{ij} \quad , \qquad \alpha_\beta \longrightarrow f_{ij}$$

$$\text{with } H_{\beta\gamma} \longrightarrow E\alpha \quad , \qquad \text{and } \gamma,\beta = 1$$

Due to the definitions of s_{ij}, b_{ij}, J_2^0, and K_2, it is evident that the functional representation of the model of plasticity developed earlier is described by the following general form of equations:

$$\dot{\varepsilon}_{ij}^{in} = \dot{\varepsilon}_{ij}^{in}\left(\sigma_{kl}, \beta_{kl}, \dot{\varepsilon}_{kl}\right) \qquad , \qquad \dot{f}_{ij} = \dot{f}_{ij}\left(\sigma_{kl}, \beta_{kl}, \dot{\varepsilon}_{kl}\right)$$

These two functional representations match the first two criteria in Eqs. (A.10). Thus the formulation set forth in Eqs. (3.19) and (3.20) is thermodynamically admissable for the development presented here. That is, for the set of thermodynamic state variables $\{\varepsilon_{ij}^{el}, \alpha_\beta, \dot{\varepsilon}_{ij}\}$, the formulation for plastic behavior of materials developed earlier (Eqs. (3.19) and (3.20) is consistent with the laws of thermodynamics.

Reference has been made earlier to the thermodynamic formulation of Freed and Chaboche [29]. The development here and the development in [29] follow the same basic lines with one notable exception. In [29] the general formulation is based upon the set of variables $\{\varepsilon_{ij}^{el}, \alpha_\beta, T, \nabla_i T\}$ as the thermodynamic state whereas in the development given here the strain rate $\dot{\varepsilon}_{ij}$ is also included as a state variable. The inclusion of $\dot{\varepsilon}_{ij}$ is not usually used as a state variable in viscoelastic or continuum damage formulations. Its appearance in the formulation results from the extension process which produced the three dimensional law (Eqs. (3.19) and (3.20)). Recall that for the problems being considered in earthquake engineering the displacements rather than the forces are specified. Therefore, its existence does not pose a problem for the solution of stresses.

NATIONAL CENTER FOR EARTHQUAKE ENGINEERING RESEARCH
LIST OF TECHNICAL REPORTS

The National Center for Earthquake Engineering Research (NCEER) publishes technical reports on a variety of subjects related to earthquake engineering written by authors funded through NCEER. These reports are available from both NCEER's Publications Department and the National Technical Information Service (NTIS). Requests for reports should be directed to the Publications Department, National Center for Earthquake Engineering Research, State University of New York at Buffalo, Red Jacket Quadrangle, Buffalo, New York 14261. Reports can also be requested through NTIS, 5285 Port Royal Road, Springfield, Virginia 22161. NTIS accession numbers are shown in parenthesis, if available.

NCEER-87-0001 "First-Year Program in Research, Education and Technology Transfer," 3/5/87, (PB88-134275/AS).

NCEER-87-0002 "Experimental Evaluation of Instantaneous Optimal Algorithms for Structural Control," by R.C. Lin, T.T. Soong and A.M. Reinhorn, 4/20/87, (PB88-134341/AS).

NCEER-87-0003 "Experimentation Using the Earthquake Simulation Facilities at University at Buffalo," by A.M. Reinhorn and R.L. Ketter, to be published.

NCEER-87-0004 "The System Characteristics and Performance of a Shaking Table," by J.S. Hwang, K.C. Chang and G.C. Lee, 6/1/87, (PB88-134259/AS). This report is available only through NTIS (see address given above).

NCEER-87-0005 "A Finite Element Formulation for Nonlinear Viscoplastic Material Using a Q Model," by O. Gyebi and G. Dasgupta, 11/2/87, (PB88-213764/AS).

NCEER-87-0006 "Symbolic Manipulation Program (SMP) - Algebraic Codes for Two and Three Dimensional Finite Element Formulations," by X. Lee and G. Dasgupta, 11/9/87, (PB88-219522/AS).

NCEER-87-0007 "Instantaneous Optimal Control Laws for Tall Buildings Under Seismic Excitations," by J.N. Yang, A. Akbarpour and P. Ghaemmaghami, 6/10/87, (PB88-134333/AS).

NCEER-87-0008 "IDARC: Inelastic Damage Analysis of Reinforced Concrete Frame - Shear-Wall Structures," by Y.J. Park, A.M. Reinhorn and S.K. Kunnath, 7/20/87, (PB88-134325/AS).

NCEER-87-0009 "Liquefaction Potential for New York State: A Preliminary Report on Sites in Manhattan and Buffalo," by M. Budhu, V. Vijayakumar, R.F. Giese and L. Baumgras, 8/31/87, (PB88-163704/AS). This report is available only through NTIS (see address given above).

NCEER-87-0010 "Vertical and Torsional Vibration of Foundations in Inhomogeneous Media," by A.S. Veletsos and K.W. Dotson, 6/1/87, (PB88-134291/AS).

NCEER-87-0011 "Seismic Probabilistic Risk Assessment and Seismic Margins Studies for Nuclear Power Plants," by Howard H.M. Hwang, 6/15/87, (PB88-134267/AS).

NCEER-87-0012 "Parametric Studies of Frequency Response of Secondary Systems Under Ground-Acceleration Excitations," by Y. Yong and Y.K. Lin, 6/10/87, (PB88-134309/AS).

NCEER-87-0013 "Frequency Response of Secondary Systems Under Seismic Excitation," by J.A. HoLung, J. Cai and Y.K. Lin, 7/31/87, (PB88-134317/AS).

NCEER-87-0014 "Modelling Earthquake Ground Motions in Seismically Active Regions Using Parametric Time Series Methods," by G.W. Ellis and A.S. Cakmak, 8/25/87, (PB88-134283/AS).

NCEER-87-0015 "Detection and Assessment of Seismic Structural Damage," by E. DiPasquale and A.S. Cakmak, 8/25/87, (PB88-163712/AS).

NCEER-87-0016 "Pipeline Experiment at Parkfield, California," by J. Isenberg and E. Richardson, 9/15/87, (PB88-163720/AS). This report is available only through NTIS (see address given above).

NCEER-87-0017 "Digital Simulation of Seismic Ground Motion," by M. Shinozuka, G. Deodatis and T. Harada, 8/31/87, (PB88-155197/AS). This report is available only through NTIS (see address given above).

NCEER-87-0018 "Practical Considerations for Structural Control: System Uncertainty, System Time Delay and Truncation of Small Control Forces," J.N. Yang and A. Akbarpour, 8/10/87, (PB88-163738/AS).

NCEER-87-0019 "Modal Analysis of Nonclassically Damped Structural Systems Using Canonical Transformation," by J.N. Yang, S. Sarkani and F.X. Long, 9/27/87, (PB88-187851/AS).

NCEER-87-0020 "A Nonstationary Solution in Random Vibration Theory," by J.R. Red-Horse and P.D. Spanos, 11/3/87, (PB88-163746/AS).

NCEER-87-0021 "Horizontal Impedances for Radially Inhomogeneous Viscoelastic Soil Layers," by A.S. Veletsos and K.W. Dotson, 10/15/87, (PB88-150859/AS).

NCEER-87-0022 "Seismic Damage Assessment of Reinforced Concrete Members," by Y.S. Chung, C. Meyer and M. Shinozuka, 10/9/87, (PB88-150867/AS). This report is available only through NTIS (see address given above).

NCEER-87-0023 "Active Structural Control in Civil Engineering," by T.T. Soong, 11/11/87, (PB88-187778/AS).

NCEER-87-0024 Vertical and Torsional Impedances for Radially Inhomogeneous Viscoelastic Soil Layers," by K.W. Dotson and A.S. Veletsos, 12/87, (PB88-187786/AS).

NCEER-87-0025 "Proceedings from the Symposium on Seismic Hazards, Ground Motions, Soil-Liquefaction and Engineering Practice in Eastern North America," October 20-22, 1987, edited by K.H. Jacob, 12/87, (PB88-188115/AS).

NCEER-87-0026 "Report on the Whittier-Narrows, California, Earthquake of October 1, 1987," by J. Pantelic and A. Reinhorn, 11/87, (PB88-187752/AS). This report is available only through NTIS (see address given above).

NCEER-87-0027 "Design of a Modular Program for Transient Nonlinear Analysis of Large 3-D Building Structures," by S. Srivastav and J.F. Abel, 12/30/87, (PB88-187950/AS).

NCEER-87-0028 "Second-Year Program in Research, Education and Technology Transfer," 3/8/88, (PB88-219480/AS).

NCEER-88-0001 "Workshop on Seismic Computer Analysis and Design of Buildings With Interactive Graphics," by W. McGuire, J.F. Abel and C.H. Conley, 1/18/88, (PB88-187760/AS).

NCEER-88-0002 "Optimal Control of Nonlinear Flexible Structures," by J.N. Yang, F.X. Long and D. Wong, 1/22/88, (PB88-213772/AS).

NCEER-88-0003 "Substructuring Techniques in the Time Domain for Primary-Secondary Structural Systems," by G.D. Manolis and G. Juhn, 2/10/88, (PB88-213780/AS).

NCEER-88-0004 "Iterative Seismic Analysis of Primary-Secondary Systems," by A. Singhal, L.D. Lutes and P.D. Spanos, 2/23/88, (PB88-213798/AS).

NCEER-88-0005 "Stochastic Finite Element Expansion for Random Media," by P.D. Spanos and R. Ghanem, 3/14/88, (PB88-213806/AS).

NCEER-88-0006 "Combining Structural Optimization and Structural Control," by F.Y. Cheng and C.P. Pantelides, 1/10/88, (PB88-213814/AS).

NCEER-88-0007 "Seismic Performance Assessment of Code-Designed Structures," by H.H-M. Hwang, J-W. Jaw and H-J. Shau, 3/20/88, (PB88-219423/AS).

NCEER-88-0008 "Reliability Analysis of Code-Designed Structures Under Natural Hazards," by H.H-M. Hwang, H. Ushiba and M. Shinozuka, 2/29/88, (PB88-229471/AS).

NCEER-88-0009 "Seismic Fragility Analysis of Shear Wall Structures," by J-W Jaw and H.H-M. Hwang, 4/30/88, (PB89-102867/AS).

NCEER-88-0010 "Base Isolation of a Multi-Story Building Under a Harmonic Ground Motion - A Comparison of Performances of Various Systems," by F-G Fan, G. Ahmadi and I.G. Tadjbakhsh, 5/18/88, (PB89-122238/AS).

NCEER-88-0011 "Seismic Floor Response Spectra for a Combined System by Green's Functions," by F.M. Lavelle, L.A. Bergman and P.D. Spanos, 5/1/88, (PB89-102875/AS).

NCEER-88-0012 "A New Solution Technique for Randomly Excited Hysteretic Structures," by G.Q. Cai and Y.K. Lin, 5/16/88, (PB89-102883/AS).

NCEER-88-0013 "A Study of Radiation Damping and Soil-Structure Interaction Effects in the Centrifuge," by K. Weissman, supervised by J.H. Prevost, 5/24/88, (PB89-144703/AS).

NCEER-88-0014 "Parameter Identification and Implementation of a Kinematic Plasticity Model for Frictional Soils," by J.H. Prevost and D.V. Griffiths, to be published.

NCEER-88-0015 "Two- and Three- Dimensional Dynamic Finite Element Analyses of the Long Valley Dam," by D.V. Griffiths and J.H. Prevost, 6/17/88, (PB89-144711/AS).

NCEER-88-0016 "Damage Assessment of Reinforced Concrete Structures in Eastern United States," by A.M. Reinhorn, M.J. Seidel, S.K. Kunnath and Y.J. Park, 6/15/88, (PB89-122220/AS).

NCEER-88-0017 "Dynamic Compliance of Vertically Loaded Strip Foundations in Multilayered Viscoelastic Soils," by S. Ahmad and A.S.M. Israil, 6/17/88, (PB89-102891/AS).

NCEER-88-0018 "An Experimental Study of Seismic Structural Response With Added Viscoelastic Dampers," by R.C. Lin, Z. Liang, T.T. Soong and R.H. Zhang, 6/30/88, (PB89-122212/AS).

NCEER-88-0019 "Experimental Investigation of Primary - Secondary System Interaction," by G.D. Manolis, G. Juhn and A.M. Reinhorn, 5/27/88, (PB89-122204/AS).

NCEER-88-0020 "A Response Spectrum Approach For Analysis of Nonclassically Damped Structures," by J.N. Yang, S. Sarkani and F.X. Long, 4/22/88, (PB89-102909/AS).

NCEER-88-0021 "Seismic Interaction of Structures and Soils: Stochastic Approach," by A.S. Veletsos and A.M. Prasad, 7/21/88, (PB89-122196/AS).

NCEER-88-0022 "Identification of the Serviceability Limit State and Detection of Seismic Structural Damage," by E. DiPasquale and A.S. Cakmak, 6/15/88, (PB89-122188/AS).

NCEER-88-0023 "Multi-Hazard Risk Analysis: Case of a Simple Offshore Structure," by B.K. Bhartia and E.H. Vanmarcke, 7/21/88, (PB89-145213/AS).

NCEER-88-0024 "Automated Seismic Design of Reinforced Concrete Buildings," by Y.S. Chung, C. Meyer and M. Shinozuka, 7/5/88, (PB89-122170/AS).

NCEER-88-0025 "Experimental Study of Active Control of MDOF Structures Under Seismic Excitations," by L.L. Chung, R.C. Lin, T.T. Soong and A.M. Reinhorn, 7/10/88, (PB89-122600/AS).

NCEER-88-0026 "Earthquake Simulation Tests of a Low-Rise Metal Structure," by J.S. Hwang, K.C. Chang, G.C. Lee and R.L. Ketter, 8/1/88, (PB89-102917/AS).

NCEER-88-0027 "Systems Study of Urban Response and Reconstruction Due to Catastrophic Earthquakes," by F. Kozin and H.K. Zhou, 9/22/88, (PB90-162348/AS).

NCEER-88-0028 "Seismic Fragility Analysis of Plane Frame Structures," by H.H-M. Hwang and Y.K. Low, 7/31/88, (PB89-131445/AS).

NCEER-88-0029 "Response Analysis of Stochastic Structures," by A. Kardara, C. Bucher and M. Shinozuka, 9/22/88, (PB89-174429/AS).

NCEER-88-0030 "Nonnormal Accelerations Due to Yielding in a Primary Structure," by D.C.K. Chen and L.D. Lutes, 9/19/88, (PB89-131437/AS).

NCEER-88-0031 "Design Approaches for Soil-Structure Interaction," by A.S. Veletsos, A.M. Prasad and Y. Tang, 12/30/88, (PB89-174437/AS).

NCEER-88-0032 "A Re-evaluation of Design Spectra for Seismic Damage Control," by C.J. Turkstra and A.G. Tallin, 11/7/88, (PB89-145221/AS).

NCEER-88-0033 "The Behavior and Design of Noncontact Lap Splices Subjected to Repeated Inelastic Tensile Loading," by V.E. Sagan, P. Gergely and R.N. White, 12/8/88, (PB89-163737/AS).

NCEER-88-0034 "Seismic Response of Pile Foundations," by S.M. Mamoon, P.K. Banerjee and S. Ahmad, 11/1/88, (PB89-145239/AS).

NCEER-88-0035 "Modeling of R/C Building Structures With Flexible Floor Diaphragms (IDARC2)," by A.M. Reinhorn, S.K. Kunnath and N. Panahshahi, 9/7/88, (PB89-207153/AS).

NCEER-88-0036 "Solution of the Dam-Reservoir Interaction Problem Using a Combination of FEM, BEM with Particular Integrals, Modal Analysis, and Substructuring," by C-S. Tsai, G.C. Lee and R.L. Ketter, 12/31/88, (PB89-207146/AS).

NCEER-88-0037 "Optimal Placement of Actuators for Structural Control," by F.Y. Cheng and C.P. Pantelides, 8/15/88, (PB89-162846/AS).

NCEER-88-0038 "Teflon Bearings in Aseismic Base Isolation: Experimental Studies and Mathematical Modeling," by A. Mokha, M.C. Constantinou and A.M. Reinhorn, 12/5/88, (PB89-218457/AS).

NCEER-88-0039 "Seismic Behavior of Flat Slab High-Rise Buildings in the New York City Area," by P. Weidlinger and M. Ettouney, 10/15/88, (PB90-145681/AS).

NCEER-88-0040 "Evaluation of the Earthquake Resistance of Existing Buildings in New York City," by P. Weidlinger and M. Ettouney, 10/15/88, to be published.

NCEER-88-0041 "Small-Scale Modeling Techniques for Reinforced Concrete Structures Subjected to Seismic Loads," by W. Kim, A. El-Attar and R.N. White, 11/22/88, (PB89-189625/AS).

NCEER-88-0042 "Modeling Strong Ground Motion from Multiple Event Earthquakes," by G.W. Ellis and A.S. Cakmak, 10/15/88, (PB89-174445/AS).

NCEER-88-0043 "Nonstationary Models of Seismic Ground Acceleration," by M. Grigoriu, S.E. Ruiz and E. Rosenblueth, 7/15/88, (PB89-189617/AS).

NCEER-88-0044 "SARCF User's Guide: Seismic Analysis of Reinforced Concrete Frames," by Y.S. Chung, C. Meyer and M. Shinozuka, 11/9/88, (PB89-174452/AS).

NCEER-88-0045 "First Expert Panel Meeting on Disaster Research and Planning," edited by J. Pantelic and J. Stoyle, 9/15/88, (PB89-174460/AS).

NCEER-88-0046 "Preliminary Studies of the Effect of Degrading Infill Walls on the Nonlinear Seismic Response of Steel Frames," by C.Z. Chrysostomou, P. Gergely and J.F. Abel, 12/19/88, (PB89-208383/AS).

NCEER-88-0047 "Reinforced Concrete Frame Component Testing Facility - Design, Construction, Instrumentation and Operation," by S.P. Pessiki, C. Conley, T. Bond, P. Gergely and R.N. White, 12/16/88, (PB89-174478/AS).

NCEER-89-0001 "Effects of Protective Cushion and Soil Compliancy on the Response of Equipment Within a Seismically Excited Building," by J.A. HoLung, 2/16/89, (PB89-207179/AS).

NCEER-89-0002 "Statistical Evaluation of Response Modification Factors for Reinforced Concrete Structures," by H.H-M. Hwang and J-W. Jaw, 2/17/89, (PB89-207187/AS).

NCEER-89-0003 "Hysteretic Columns Under Random Excitation," by G-Q. Cai and Y.K. Lin, 1/9/89, (PB89-196513/AS).

NCEER-89-0004 "Experimental Study of 'Elephant Foot Bulge' Instability of Thin-Walled Metal Tanks," by Z-H. Jia and R.L. Ketter, 2/22/89, (PB89-207195/AS).

NCEER-89-0005 "Experiment on Performance of Buried Pipelines Across San Andreas Fault," by J. Isenberg, E. Richardson and T.D. O'Rourke, 3/10/89, (PB89-218440/AS).

NCEER-89-0006 "A Knowledge-Based Approach to Structural Design of Earthquake-Resistant Buildings," by M. Subramani, P. Gergely, C.H. Conley, J.F. Abel and A.H. Zaghw, 1/15/89, (PB89-218465/AS).

NCEER-89-0007 "Liquefaction Hazards and Their Effects on Buried Pipelines," by T.D. O'Rourke and P.A. Lane, 2/1/89, (PB89-218481).

NCEER-89-0008 "Fundamentals of System Identification in Structural Dynamics," by H. Imai, C-B. Yun, O. Maruyama and M. Shinozuka, 1/26/89, (PB89-207211/AS).

NCEER-89-0009 "Effects of the 1985 Michoacan Earthquake on Water Systems and Other Buried Lifelines in Mexico," by A.G. Ayala and M.J. O'Rourke, 3/8/89, (PB89-207229/AS).

NCEER-89-R010 "NCEER Bibliography of Earthquake Education Materials," by K.E.K. Ross, Second Revision, 9/1/89, (PB90-125352/AS).

NCEER-89-0011 "Inelastic Three-Dimensional Response Analysis of Reinforced Concrete Building Structures (IDARC-3D), Part I - Modeling," by S.K. Kunnath and A.M. Reinhorn, 4/17/89, (PB90-114612/AS).

NCEER-89-0012 "Recommended Modifications to ATC-14," by C.D. Poland and J.O. Malley, 4/12/89, (PB90-108648/AS).

NCEER-89-0013 "Repair and Strengthening of Beam-to-Column Connections Subjected to Earthquake Loading," by M. Corazao and A.J. Durrani, 2/28/89, (PB90-109885/AS).

NCEER-89-0014 "Program EXKAL2 for Identification of Structural Dynamic Systems," by O. Maruyama, C-B. Yun, M. Hoshiya and M. Shinozuka, 5/19/89, (PB90-109877/AS).

NCEER-89-0015 "Response of Frames With Bolted Semi-Rigid Connections, Part I - Experimental Study and Analytical Predictions," by P.J. DiCorso, A.M. Reinhorn, J.R. Dickerson, J.B. Radziminski and W.L. Harper, 6/1/89, to be published.

NCEER-89-0016 "ARMA Monte Carlo Simulation in Probabilistic Structural Analysis," by P.D. Spanos and M.P. Mignolet, 7/10/89, (PB90-109893/AS).

NCEER-89-P017 "Preliminary Proceedings from the Conference on Disaster Preparedness - The Place of Earthquake Education in Our Schools," Edited by K.E.K. Ross, 6/23/89.

NCEER-89-0017 "Proceedings from the Conference on Disaster Preparedness - The Place of Earthquake Education in Our Schools," Edited by K.E.K. Ross, 12/31/89, (PB90-207895).

NCEER-89-0018 "Multidimensional Models of Hysteretic Material Behavior for Vibration Analysis of Shape Memory Energy Absorbing Devices, by E.J. Graesser and F.A. Cozzarelli, 6/7/89, (PB90-164146/AS).

NCEER-89-0019 "Nonlinear Dynamic Analysis of Three-Dimensional Base Isolated Structures (3D-BASIS)," by S. Nagarajaiah, A.M. Reinhorn and M.C. Constantinou, 8/3/89, (PB90-161936/AS).

NCEER-89-0020 "Structural Control Considering Time-Rate of Control Forces and Control Rate Constraints," by F.Y. Cheng and C.P. Pantelides, 8/3/89, (PB90-120445/AS).

NCEER-89-0021 "Subsurface Conditions of Memphis and Shelby County," by K.W. Ng, T-S. Chang and H-H.M. Hwang, 7/26/89, (PB90-120437/AS).

NCEER-89-0022 "Seismic Wave Propagation Effects on Straight Jointed Buried Pipelines," by K. Elhmadi and M.J. O'Rourke, 8/24/89, (PB90-162322/AS).

NCEER-89-0023 "Workshop on Serviceability Analysis of Water Delivery Systems," edited by M. Grigoriu, 3/6/89, (PB90-127424/AS).

NCEER-89-0024 "Shaking Table Study of a 1/5 Scale Steel Frame Composed of Tapered Members," by K.C. Chang, J.S. Hwang and G.C. Lee, 9/18/89, (PB90-160169/AS).

NCEER-89-0025 "DYNA1D: A Computer Program for Nonlinear Seismic Site Response Analysis - Technical Documentation," by Jean H. Prevost, 9/14/89, (PB90-161944/AS).

NCEER-89-0026 "1:4 Scale Model Studies of Active Tendon Systems and Active Mass Dampers for Aseismic Protection," by A.M. Reinhorn, T.T. Soong, R.C. Lin, Y.P. Yang, Y. Fukao, H. Abe and M. Nakai, 9/15/89, (PB90-173246/AS).

NCEER-89-0027 "Scattering of Waves by Inclusions in a Nonhomogeneous Elastic Half Space Solved by Boundary Element Methods," by P.K. Hadley, A. Askar and A.S. Cakmak, 6/15/89, (PB90-145699/AS).

NCEER-89-0028 "Statistical Evaluation of Deflection Amplification Factors for Reinforced Concrete Structures," by H.H.M. Hwang, J-W. Jaw and A.L. Ch'ng, 8/31/89, (PB90-164633/AS).

NCEER-89-0029 "Bedrock Accelerations in Memphis Area Due to Large New Madrid Earthquakes," by H.H.M. Hwang, C.H.S. Chen and G. Yu, 11/7/89, (PB90-162330/AS).

NCEER-89-0030 "Seismic Behavior and Response Sensitivity of Secondary Structural Systems," by Y.Q. Chen and T.T. Soong, 10/23/89, (PB90-164658/AS).

NCEER-89-0031 "Random Vibration and Reliability Analysis of Primary-Secondary Structural Systems," by Y. Ibrahim, M. Grigoriu and T.T. Soong, 11/10/89, (PB90-161951/AS).

NCEER-89-0032 "Proceedings from the Second U.S. - Japan Workshop on Liquefaction, Large Ground Deformation and Their Effects on Lifelines, September 26-29, 1989," Edited by T.D. O'Rourke and M. Hamada, 12/1/89, (PB90-209388/AS).

NCEER-89-0033 "Deterministic Model for Seismic Damage Evaluation of Reinforced Concrete Structures," by J.M. Bracci, A.M. Reinhorn, J.B. Mander and S.K. Kunnath, 9/27/89.

NCEER-89-0034 "On the Relation Between Local and Global Damage Indices," by E. DiPasquale and A.S. Cakmak, 8/15/89, (PB90-173865).

NCEER-89-0035 "Cyclic Undrained Behavior of Nonplastic and Low Plasticity Silts," by A.J. Walker and H.E. Stewart, 7/26/89, (PB90-183518/AS).

NCEER-89-0036 "Liquefaction Potential of Surficial Deposits in the City of Buffalo, New York," by M. Budhu, R. Giese and L. Baumgrass, 1/17/89, (PB90-208455/AS).

NCEER-89-0037 "A Determinstic Assessment of Effects of Ground Motion Incoherence," by A.S. Veletsos and Y. Tang, 7/15/89, (PB90-164294/AS).

NCEER-89-0038 "Workshop on Ground Motion Parameters for Seismic Hazard Mapping," July 17-18, 1989, edited by R.V. Whitman, 12/1/89, (PB90-173923/AS).

NCEER-89-0039 "Seismic Effects on Elevated Transit Lines of the New York City Transit Authority," by C.J. Costantino, C.A. Miller and E. Heymsfield, 12/26/89, (PB90-207887/AS).

NCEER-89-0040 "Centrifugal Modeling of Dynamic Soil-Structure Interaction," by K. Weissman, Supervised by J.H. Prevost, 5/10/89, (PB90-207879/AS).

NCEER-89-0041 "Linearized Identification of Buildings With Cores for Seismic Vulnerability Assessment," by I-K. Ho and A.E. Aktan, 11/1/89.

NCEER-90-0001 "Geotechnical and Lifeline Aspects of the October 17, 1989 Loma Prieta Earthquake in San Francisco," by T.D. O'Rourke, H.E. Stewart, F.T. Blackburn and T.S. Dickerman, 1/90, (PB90-208596/AS).

NCEER-90-0002 "Nonnormal Secondary Response Due to Yielding in a Primary Structure," by D.C.K. Chen and L.D. Lutes, 2/28/90.

NCEER-90-0003 "Earthquake Education Materials for Grades K-12," by K.E.K. Ross, 4/16/90.

NCEER-90-0004 "Catalog of Strong Motion Stations in Eastern North America," by R.W. Busby, 4/3/90.

NCEER-90-0005 "NCEER Strong-Motion Data Base: A User Manuel for the GeoBase Release (Version 1.0 for the Sun3)," by P. Friberg and K. Jacob, 3/31/90.

NCEER-90-0006 "Seismic Hazard Along a Crude Oil Pipeline in the Event of an 1811-1812 Type New Madrid Earthquake," by H.H.M. Hwang and C-H.S. Chen, 4/16/90.

NCEER-90-0007 "Site-Specific Response Spectra for Memphis Sheahan Pumping Station," by H.H.M. Hwang and C.S. Lee, 5/15/90.

NCEER-90-0008 "Pilot Study on Seismic Vulnerability of Crude Oil Transmission Systems," by T. Ariman, R. Dobry, M. Grigoriu, F. Kozin, M. O'Rourke, T. O'Rourke and M. Shinozuka, 5/25/90.

NCEER-90-0009 "A Program to Generate Site Dependent Time Histories: EQGEN," by G.W. Ellis, M. Srinivasan and A.S. Cakmak, 1/30/90.

NCEER-90-0010 "Active Isolation for Seismic Protection of Operating Rooms," by M.E. Talbott, Supervised by M. Shinozuka, 6/8/9.

NCEER-90-0011 "Program LINEARID for Identification of Linear Structural Dynamic Systems," by C-B. Yun and M. Shinozuka, 6/25/90.

NCEER-90-0012 "Two-Dimensional Two-Phase Elasto-Plastic Seismic Response of Earth Dams," by A.N. Yiagos, Supervised by J.H. Prevost, 6/20/90.

NCEER-90-0013 "Secondary Systems in Base-Isolated Structures: Experimental Investigation, Stochastic Response and Stochastic Sensitivity," by G.D. Manolis, G. Juhn, M.C. Constantinou and A.M. Reinhorn, 7/1/90.

NCEER-90-0014 "Seismic Behavior of Lightly-Reinforced Concrete Column and Beam-Column Joint Details," by S.P. Pessiki, C.H. Conley, P. Gergely and R.N. White, 8/22/90.

NCEER-90-0015 "Two Hybrid Control Systems for Building Structures Under Strong Earthquakes," by J.N. Yang and A. Danielians, 6/29/90.

NCEER-90-0016 "Instantaneous Optimal Control with Acceleration and Velocity Feedback," by J.N. Yang and Z. Li, 6/29/90.

NCEER-90-0017 "Reconnaissance Report on the Northern Iran Earthquake of June 21, 1990," by M. Mehrain, 10/4/90.

NCEER-90-0018 "Evaluation of Liquefaction Potential in Memphis and Shelby County," by T.S. Chang, P.S. Tang, C.S. Lee and H. Hwang, 8/10/90.

NCEER-90-0019 "Experimental and Analytical Study of a Combined Sliding Disc Bearing and Helical Steel Spring Isolation System," by M.C. Constantinou, A.S. Mokha and A.M. Reinhorn, 10/4/90.

NCEER-90-0020 "Experimental Study and Analytical Prediction of Earthquake Response of a Sliding Isolation System with a Spherical Surface," by A.S. Mokha, M.C. Constantinou and A.M. Reinhorn, 10/11/90.

NCEER-90-0021 "Dynamic Interaction Factors for Floating Pile Groups," by G. Gazetas, K. Fan, A. Kaynia and E. Kausel, 9/10/90.

NCEER-90-0022 "Evaluation of Seismic Damage Indices for Reinforced Concrete Structures," by S. Rodríguez-Gómez and A.S. Cakmak, 9/30/90.

NCEER-90-0023 "Study of Site Response at a Selected Memphis Site," by H. Desai, S. Ahmad, E.S. Gazetas and M.R. Oh, 10/11/90.

NCEER-90-0024 "A User's Guide to Strongmo: Version 1.0 of NCEER's Strong-Motion Data Access Tool for PCs and Terminals," by P.A. Friberg and C.A.T. Susch, 11/15/90.

NCEER-90-0025 "A Three-Dimensional Analytical Study of Spatial Variability of Seismic Ground Motions," by L-L. Hong and A.H.-S. Ang, 10/30/90.

NCEER-90-0026 "MUMOID User's Guide - A Program for the Identification of Modal Parameters," by S. Rodríguez-Gómez and E. DiPasquale, 9/30/90.

NCEER-90-0027 "SARCF-II User's Guide - Seismic Analysis of Reinforced Concrete Frames," by S. Rodríguez-Gómez, Y.S. Chung and C. Meyer, 9/30/90.

NCEER-90-0028 "Viscous Dampers: Testing, Modeling and Application in Vibration and Seismic Isolation," by N. Makris and M.C. Constantinou, 12/20/90.

NCEER-90-0029 "Soil Effects on Earthquake Ground Motions in the Memphis Area," by H. Hwang, C.S. Lee, K.W. Ng and T.S. Chang, 8/2/90.

NCEER-91-0001 "Proceedings from the Third Japan-U.S. Workshop on Earthquake Resistant Design of Lifeline Facilities and Countermeasures for Soil Liquefaction, December 17-19, 1990," edited by T.D. O'Rourke and M. Hamada, 2/1/91.

NCEER-91-0002 "Physical Space Solutions of Non-Proportionally Damped Systems," by M. Tong, Z. Liang and G.C. Lee, 1/15/91.

NCEER-91-0003 "Kinematic Seismic Response of Single Piles and Pile Groups," by K. Fan, G. Gazetas, A. Kaynia, E. Kausel and S. Ahmad, 1/10/91.

NCEER-91-0004 "Theory of Complex Damping," by Z. Liang and G. Lee, to be published.

NCEER-91-0005 "3D-BASIS - Nonlinear Dynamic Analysis of Three Dimensional Base Isolated Structures: Part II," by S. Nagarajaiah, A.M. Reinhorn and M.C. Constantinou, 2/28/91.

NCEER-91-0006 "A Multidimensional Hysteretic Model for Plasticity Deforming Metals in Energy Absorbing Devices," by E.J. Graesser and F.A. Cozzarelli, 4/9/91.